

DEVELOPMENT OF A THICKNESS GAUGE FOR MEASURING  
THIN MATERIALS

by

A.CİHAT BAYTAŞ

B.S in M.E., Yıldız University, 1981

Submitted to the Institute for Graduate Studies in  
Science and Engineering in partial fulfillment of  
the requirements for the degree of

Master of Science

in

Nuclear Engineering

Bogazici University Library



39001100315145

14

Boğaziçi University

1984

## ACKNOWLEDGEMENTS

I am grateful to Doc. Dr. A.Nezihi BİLGE for his supervision. I am also grateful to Prof. Dr. Turan B. ENGİNOĞLU and Doc. Dr. Vural ALTIN from Boğaziçi University for their valuable suggestions and stimulating discussions at the later stage of the thesis.

I wish to thank Mrs. Işıl ALKAN, the head of Industrial Application Department, and Dr. Fadıl AKGÜN, Çekmece Nuclear Research and Training Center, for providing the facilities for this work. Thanks are also due to members of the Industrial Application Department. They were always ready to help.

## ABSTRACT

Thickness gauges using nuclear techniques and radioactive sources are devised to measure the material thicknesses of the order of microns in a non-destructive manner without contacting the material. This allows for quality control by measuring the thickness during production and adjustment of the system in the case of a failure.

The thickness gauge which is the subject of my thesis study is designed to use gamma transmission method. In the transmission method, the set-up consists of the detector and the radioactive source placed at opposite sides of the material whose thickness is to be measured.

Unknown thicknesses can be found by using this thickness gauge with the aid of calibration curves that have been prepared according to the source and the geometry used.

Minimum detection limits of various materials that can be measured with this gauge have also been determined so as to give an idea about the accuracy of the gauge.

## ÖZET

Nükleer teknikler yardımı ile ve radyoaktif kaynak kullanılarak yapılan kalınlık ölçme cihazının amacı mikron mertebesinde malzemelerin kalınlıklarını ona temas etmeden ve malzemeyi herhangi bir şekilde tahrip etmeden kalınlığının ölçülmesine imkan tanımaktır. Bu şekilde endüstride üretim esnasında malzemenin kalınlığı ölçülerek kalite kontrolu yapılabilir ve üretim tezgahı eğer bir aksaklık varsa hemen ayarlanabilir.

Gerçekleştirilen kalınlık ölçme cihazı gamma transmisyon metoduna göre dizayn edilmiştir. Transmisyon metodunda, sistem bir tarafta dedektör, ortada ölçülecek örnek ve diğer yanda radyoaktif kaynak üçlüsünden oluşmaktadır.

Çeşitli malzemelerin bilinmeyen kalınlıkları hazırlanan kalibrasyon eğrileri yardımı ile bulunabilir. Bu eğriler kullanılan radyoaktif kaynak ve transmisyon geometrisine göre hazırlanmıştır.

Ayrıca her malzeme için kalınlık ölçme cihazının minimum kalınlık ölçme sınırı tespit edilmiş ve bu şekilde cihazın minimum ölçme kabiliyeti hakkında bir fikir edinilmiştir.

## TABLE OF CONTENTS

	page
ACKNOWLEDGEMENTS	ii
ABSTRACT	iii
ÖZET	iv
LIST OF FIGURES	vii
LIST OF TABLES	ix
LIST OF SYMBOLS	x
I. INTRODUCTION	1
1.1 GENERAL	1
II. THEORY	5
2.1 GAMMA AND X-RADIATION	5
2.2 GAMMA RAY INTERACTION WITH MATTER	7
2.2.1 PHOTOELECTRIC EFFECT	10
2.2.2 COMPTON EFFECT	10
2.2.3 PAIR PRODUCTION	11
2.3 GAMMA RADIATION SOURCES	12
III. DESIGN AND OPTIMIZATION OF A RADIOGAUGE	13
3.1 CHOICE OF RADIOGAUGE PRINCIPLE	13
3.2 CHOICE OF RADIOISOTOPE	14
IV. EXPERIMENTS AND CALCULATIONS	17
4.1 EXPERIMENTAL PROCEDURE	17
4.1.1 EXPLANATION OF ELECTRONIC AND GEOMETRIC ARRANGEMENTS	17
4.1.2 CALCULATIONS OF SOURCE INTENSITY RELATIVE TRANSMISSION GEOMETRY	21

4.1.3 DETERMINATION OF GAMMA RAY SPECTRUM	
ANALYSIS AND ENERGY CALIBRATION	24
4.1.4 EXPERIMENTAL MEASUREMENTS	34
V. MINIMUM DETECTION LIMITS	50
VI. DISCUSSION AND CONCLUSIONS	53
APPENDIX A	57
REFERENCES	68

## LIST OF FIGURES

	<u>page</u>
FIGURE 1.1 Comparison of the penetration depths of alpha,beta particles and gamma rays through air,paper,aluminium sheet and steel plate	3
FIGURE 2.1 The relative importance of the three major types of gamma ray interactions	9
FIGURE 4.1 The schematic electronic arrangement for gamma ray spectrum analysis	17
FIGURE 4.2 Geometric arrangement of collimation of a source-detector	19
FIGURE 4.3 Prototype system for thickness measurements	20
FIGURE 4.4 Schematic representation of a point source and cylindrical detector arrangement	21
FIGURE 4.5 A monoenergetic gamma ray spectrum	24
FIGURE 4.6 Determination of study voltage	28

FIGURE 4.7	The monoenergetic gamma ray spectrum for Am-241	29
FIGURE 4.8	The monoenergetic gamma ray spectrum for Cd-109	30
FIGURE 4.9	The monoenergetic gamma ray spectrum for Pu-238	31
FIGURE 4.10	Energy calibration curve	32
FIGURE 4.11	F.W.H.M. vs. source energy	33
FIGURE 4.12	Theoretical and experimental thickness calibration curves	37-50



## LIST OF TABLES

	<u>page</u>
TABLE 4.1 List of source activity	22
TABLE 4.2 Theoretical intensity from(Eq 4.2)	23
TABLE 4.3 Properties of the sources	25
TABLE 4.4 Results according to the gamma source used in the experiments	26
TABLE 4.5 Goodfellow metals	27
TABLE 4.6 Experimental results with radioactive sources	35
TABLE 5.1 Minimum detection limits( $\mu\text{m}$ )	51
TABLE 5.2 Total mass attenuation coefficient for sources and samples ( $\text{cm}^2/\text{g}$ )	52

## LIST OF SYMBOLS

$A_c$	Source activity
$D$	Distance between source and detector
$E$	Source energy
$E_b$	Binding energy of an electron
$E_e$	Kinetic energy of a emitted electron
$E_\gamma$	Gamma photon energy
$f_G$	Geometric factor of the transmission geometry
$h$	Planck's constant
$I(0)$	Counting rate with no absorber
$I(x)$	Counting rate with absorber
$K$	Detector diameter
$n$	The number of scatterers per unit volume
$R$	Orifice diameter
$s$	Sensitivity
$\lambda$	Wavelength
$\mu$	Total mass attenuation coefficient
$\nu$	Frequency
$\rho$	Density of samples
$\sigma(x)$	Standard deviation
$\tau$	Rate meter time constant
$x$	Thickness of samples

## I.. INTRODUCTION

### 1.1. GENERAL

In 1900's Becquerel first detected the radiations from a radioactive ore by after having placed a lump of ore-bearing rock against a photographic plate and finding that the film became blackened by the rays. Today industry widely utilizes the alpha, beta and gamma radiations from radioactive materials in many different fields.

Some examples of the radioisotope applications are agriculture and agricultural engineering, aircraft, building materials, chemical industries, civil engineering, coal and coke, drugs and pharmaceuticals, electrical engineering, explosives, food, paper and printing industry, photography and cinematography.

Radiation gauging is a branch of non-destructive testing which has been applied to quality control measurements of components or assemblies since about 1950's. Basically a radiation gauge consists of a radiation source, radiation detector and the related electronic equipment. Of the many radiation techniques available for component inspection, three types of measurements are

widely used, transmission, scattering and X-ray fluorescence, each requiring the use of radioisotopes.

Radioactive isotopes are valuable to solve industrial problems since;

- They are self contained sources of energy and do not require any power supplies.
- The radiations from them are easily detected.
- Their performance is unaffected by heat, pressure and vibration.
- Their properties are perfectly reproducible; i.e.

the same radioisotope always has the same properties

In addition, based on three major properties of their radiation, radioisotopes diverse applications can be divided into three groups (Gr-67).

a) Since radiation can be detected with extremely high sensitivity, radioisotopes are useful as tracers.

b) Ionization and excitation effects of their radiation make possible such uses as: dissipating electrostatic charge, improving operation of electronic gas tubes, and exciting phosphors to produce light.

c) Radiation emitted by some radioisotopes penetrates great distances in solid materials, a steel casting, for example, opening an immense field of gaging, radiography, density, thickness, level, etc. measurements, and the location of hidden objects.

The scope for use of radioisotopes in solving industrial problems has been increased greatly since their production began in nuclear reactors. This is because of the possibility of reactor irradiations to produce a wider

choice of radioactive materials than before, and because this wide range of choices enables a source of radiation to be selected which will give both the type of radiation and the length of half-life required. In choosing a radioisotope the first consideration is usually the degree of penetration required. Types of radiation available are principally gamma rays, beta particles and alpha particles which have the powers of penetration indicated in fig.(1.1).

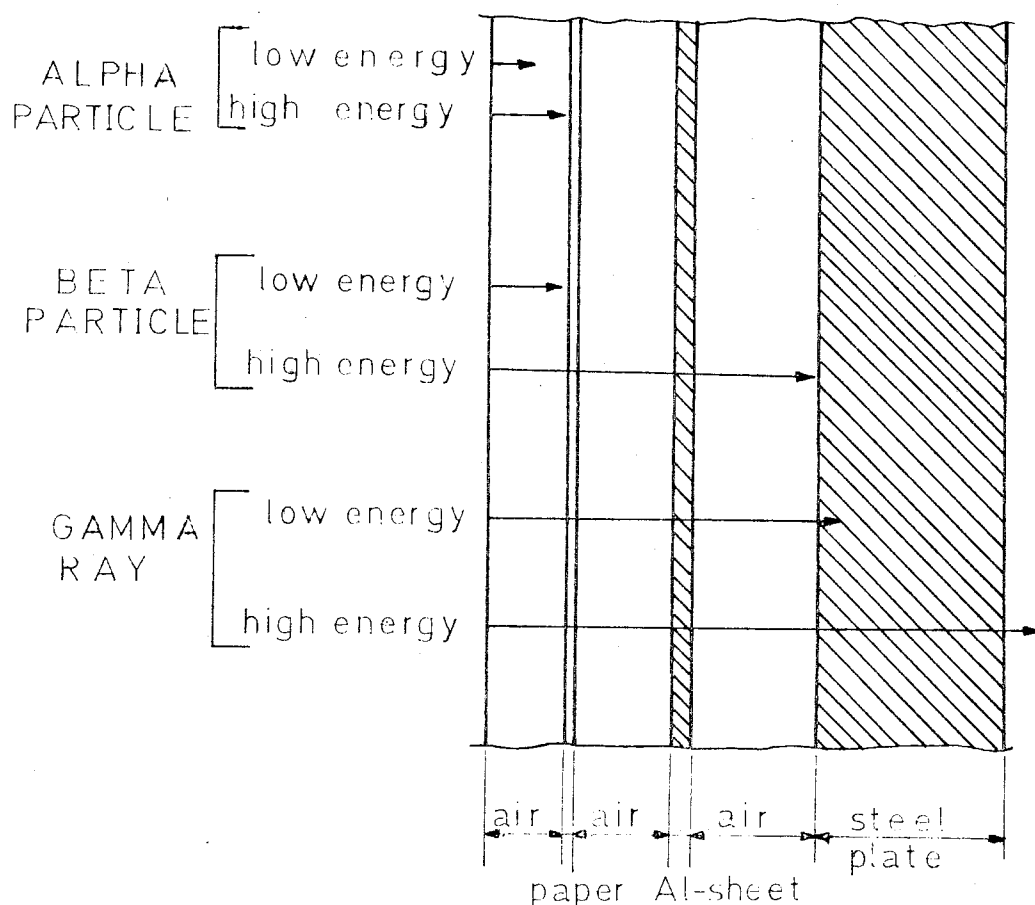


Fig. 1.1. Comparison of the penetration depths of alpha, beta particles and gamma rays through air, paper, aluminium sheet and steel plate.(Gr-67)

It will be seen that there is a range of penetration for each type of radiation depending on the energy level.

The subject of our study is thickness gauges for measuring thin materials by using the transmission technique. It is a non-destructive testing technique with which thin materials thicknesses can be measured in microns.

## II. THEORY

### 2.1. GAMMA AND X- RADIATION

Gamma rays were discovered very early among the radiations emitted by nuclei and their electromagnetic nature was established at the same time as that of X-rays (Von lave,1912). Thereafter the study of gamma rays has always played an important role in nuclear physics. Gamma rays and X-rays are electromagnetic radiations like radio signals, radiant heat and light. Discrete quanta of electromagnetic radiation are called photons and the wave nature of these photons is characterized by frequency,  $\nu$  or wavelength,  $\lambda$ . The relation among photon energy, frequency and wavelength is given in terms of Planck's constant,  $h$ , and the speed of light  $c$ ,

$$E = h\nu = hc/\lambda \quad (2.1)$$

Electromagnetic radiation can have extremely high frequencies and short wavelengths. An excited nucleus can result from a radioactive decay process when a beta or alpha particle is emitted or when electron capture occurs.

Most nuclei are left in an excited state after one of these events. The gamma radiation that is emitted represents the energy difference between one excited level of the nucleus and another energy level. In some cases the excited nucleus may go to the ground state in steps through two or more successively lower energy states, emitting gamma radiations in cascade before reaching the ground level. X-rays originate in the electron shell of the atom and is emitted when an atom goes from one energy state to a lower one. For example, when a K-shell electron has been removed, the atom is left in an excited state. The electron can be replaced by an electron from one of the outer shells, principally an L-shell electron. When this occurs, a photon of X-radiation is emitted that has an energy equal to the difference in the binding energies of the K and L shell electrons. These emitted photons of X-radiation are discrete for each electron transition.

In this study, we are concerned with the interaction of electromagnetic radiation with matter rather than origin or formation of the gamma and X-radiation.



## 2.2. GAMMA RAY INTERACTIONS WITH MATTER

Attenuation of gamma rays would be relatively simple if the interaction processes were purely absorptive, in other words, if each collision resulted in the disappearance of a photon. Thus, consider a plane gamma ray beam in such an absorptive medium. If the flux density of the beam at any point  $x$  is  $I(x)$ , then the number of collisions made in a path length  $dx$  by photons passing in unit time through a unit cross-sectional area of the beam is

$$I \sigma n dx = I \mu dx \quad (2.2)$$

where  $\sigma$  is the collision cross section of the photons per scatterer,  $n$  is the number of scatterers per unit volume, and  $\mu$  equal to  $n\sigma$ , is known as the macroscopic absorption coefficient of the medium. Since the collisions are purely absorptive, this number of collisions must be exactly equal to the decrease in the flux density  $I(0)$  over the distance  $dx$ :

$$-dI = I \mu dx \quad \text{or} \quad \frac{dI}{dx} = -\mu I \quad (2.3)$$

This simple differential equation above gives the well known Lambert's law of absorption (Go-56) :

$$I(x) = I(0) e^{-\mu x} \quad (2.4)$$

Similar expressions can be obtained for other geometries of the incident beam or source; in all of them the essential features of the attenuation will be determined by the exponential factor. However, gamma-ray interaction processes are not always completely absorptive. Sometimes the photon survives the collision with, at most, changes in direction and energy, in other words, the interaction is a scattering event rather than absorption. Even when a photon disappears on collision, the electrons or positrons resulting from the reaction may produce other photons through secondary processes. Equation (2.2) still gives the number of collisions in distance  $dx$ , but this is no longer the decrease in the flux density. The attenuation of the total beam is thus not described by Eq.(2.4), although the equation itself can be retained for the flux density of those photons which survive without having made any collisions at all. The major problem of concern in gamma-ray attenuation is to find, by experiment or theory, the number of photons which reach the observation point after one or more collisions.

For interaction of gamma rays, although a large number of possible interaction mechanisms are known for gamma rays in matter, only three major types play an important role in interaction with matter. They are photoelectric effect, Compton effect, pair production. All of these processes lead to the partial or complete transfer of the gamma ray photon energy to electron energy. There are other processes contributing to the total mass attenuation coefficient. Their effect is, however, minor.

Interaction of gamma rays with matter is shown in fig.(2.1)

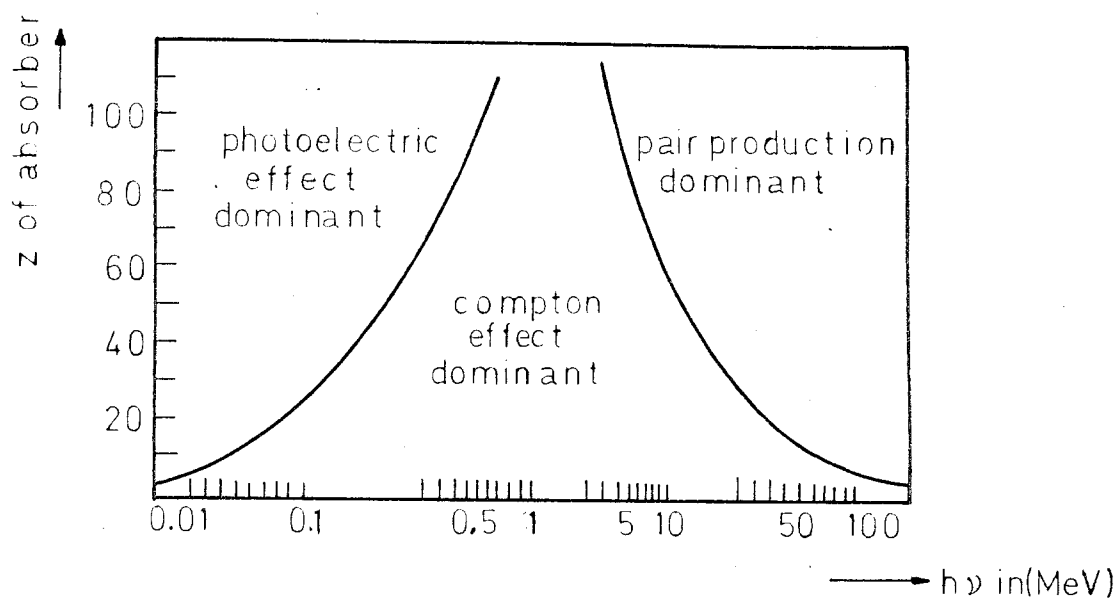


Fig. 2.1. The relative importance of the three major types of gamma ray interactions. The lines show the values of  $z$  and  $h\nu$  for which the two neighboring effects are just equal.(Kn-79)

### 2.2.1. PHOTOELECTRIC EFFECT

In the atomic photoelectric effect an incident photon transfers all its energy to one of the atomic electrons, ejecting it from the atom. The kinetic energy of the emitted electron is equal to the incident photon energy less the ionization energy of the electron. Hence the photoelectric process can occur with a given atomic electron only if the energy of the photon is greater than the electron binding energy.

$$E_e = h\nu - E_b \quad (2.5)$$

where  $E_e$  is the kinetic energy of the emitted electron,  $h\nu$  is incident photon energy,  $E_b$  is binding energy of the photoelectron.

### 2.2.2. COMPTON EFFECT

In Compton scattering, the incident photon encounters an orbital electron, loses only part of its energy in freeing that electron from its atom, and is scattered away from the beam with less energy than it initially had. It can thus be reasoned that Compton scattering becomes important at higher photon energies than the photoelectric effect.

### 2.2.3. PAIR PRODUCTION

In pair production all the energy of the incident photon is transformed into creating an electron pair—an electron and a positron. The kinetic energy of the pair is equal to the photon energy less  $2mc^2$ , the rest mass of the pair. Hence pair production has a threshold at  $2mc^2 = 1.022(\text{MeV})$  below which it cannot take place. Like the photoelectric effect, pair production cannot take place in free space; to conserve momentum it can occur only in the electric field of a particle which can carry away some of the momentum in the recoil. Either the atomic electrons or the charge on the nucleus can provide this field.

$$E^+ + E^- = h\nu - 2mc^2 \quad (2.6)$$

$$E^+ + E^- = h\nu - 1.02 (\text{MeV}) \quad (2.7)$$

If  $E^+$  is the kinetic energy of the positron,  $E^-$  is the kinetic energy of the electron, and  $2mc^2$  is the rest mass equivalent energy of the two particles; then an energy balance yields.

### 2.3. GAMMA RADIATION SOURCES

The transmission of electromagnetic radiation has been successfully used in the measurement of the thickness of metal sheets, and in the other applications.

Although a large number of radioisotopes are available as sources of electromagnetic radiation, only a relatively few are extensively used. The factors governing possible uses are availability, cost and long enough half-life.

### III. DESIGN AND OPTIMIZATION OF A RADIOGAUGE

#### 3.1. CHOICE OF RADIOGAUGE PRINCIPLE

There are several choices of radiogauge principles for the measurement of any given parameter .The optimum principle depends not only upon the accuracy that is desired but also upon such practical considerations as

- 1- availability of a suitable radioisotope source,
- 2- cost of the radiogauge system,
- 3- freedom from measurement interferences,
- 4- radiation safety considerations.

These practical factors can be treated by a common-sense approach.The choice of principle is treated here primarily from the standpoint of accuracy or sensitivity.The most common applications have been measurements of density, thickness,level of filling and component analysis. These measurements can further be classified according to the state of the sample being measured,gas,liquid and solid.

Gamma rays affected by several centimeters of liquid or solid material and are the natural choice for samples of this form and size.X-rays are available in a wide range of energies and therefore quite versatile in application.

### 3.2. CHOICE OF RADIOISOTOPE

The most important factors in the choice of a radioisotope are availability, cost, half-life and energy of emitted radiation. Especially, radiogauging principle that is quite common is the transmission of beta, gamma and X-rays through matter. For this case, one can derive the optimum mass attenuation coefficient determined by energy based on the best accuracy. The intensity of radiation passing through an absorber is given by an exponential law. For gamma and X-ray sources this law is exact for mono-energetic particles.

In terms of counting rates, this law;

$$I(x) = I(0) e^{-\mu x} \quad (3.1)$$

where  $I(x)$  is counting rate with absorber  $x$  between source and detector,  $I(0)$  is counting rate with no absorber,

$\mu$  is total mass attenuation coefficient ( $\text{cm}^2/\text{gm}$ )

$x$  is absorber density thickness ( $\text{gm}/\text{cm}^2$ )

Equation (3.1.) describes the case of the source-detector absorber arrangement shown in fig.(4.2)

To determine the optimum source for any material thickness:

Consider the definition of the standard deviation of the measured variable. For error propagation of Eq.(3.1)

$$\sigma(I(x)) = \frac{\partial I(x)}{\partial x} \sigma(x) \quad (3.1)$$



where  $\sigma(x)$  is the standard deviation of the measured values,  
 $\sigma(I(x))$  is the standard deviation of counting rate.

$$\sigma(I(x)) = \sqrt{\frac{I(x)}{2\tau}} \quad (3.3)$$

where  $\tau$  is equal to RC, the rate-meter time constant  
 R is resistance and C capacitance of the capacitor  
 of the counting rate meter.

$$\sigma(x) = \frac{\partial x}{\partial I(x)} \sigma(I(x)) \quad (3.4)$$

$$\sigma(x) = \frac{e^{-\mu x}}{\mu I(0)} \sqrt{\frac{I(x)}{2\tau}} \quad (3.5)$$

$$\sigma(x) = \frac{e^{-\mu x/2}}{\mu} \sqrt{\frac{1}{2I(0)\tau}} \quad (3.6)$$

A stationary value of the standard deviation with respect  
 to the total mass attenuation coefficient  $\mu$  is obtained  
 by the usual procedure of setting the first derivative  
 equal to zero.

$$\frac{d\sigma(x)}{d\mu} = 0 = \frac{1}{(2I(0)\tau)^{1/2}} \left[ -\frac{x}{2} \mu e^{-\mu x/2} + e^{-\mu x/2} \right] \frac{1}{\mu^2} \quad (3.7)$$

from which

$$\sqrt{Mx} = 2 \quad (3.8)$$

In this condition, standard deviation will be minimum for  $\sqrt{Mx} = 2$  (Ga-67). If the statistical counting rate fluctuation is the predominant source of error, the best accuracy will be obtained in the vicinity of Eq.(3.8).

This criterion can be used in the choice of a radioisotope source when the radiogauge operates on the exponential absorption law.

#### IV. EXPERIMENTS AND CALCULATIONS

##### 4.1. EXPERIMENTAL PROCEDURE

##### 4.1.1. Explanation of electronic and geometric arrangements

Firstly, the gamma ray spectrum is determined by using a scintillation detector which employs the electronic arrangement of fig. (4.1) and geometric arrangement of fig. (4.2).

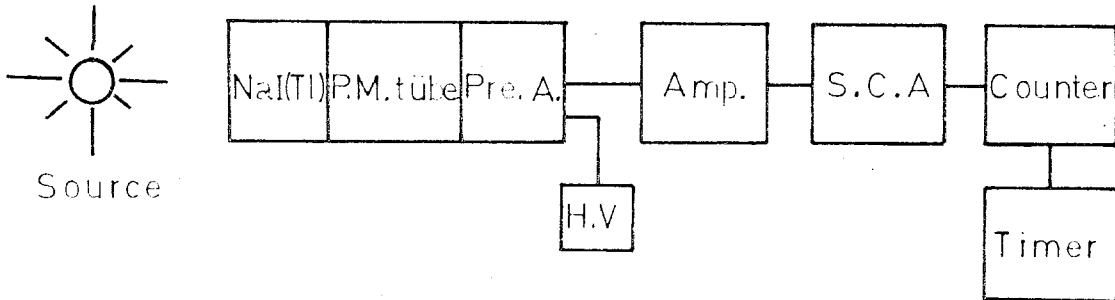


Fig. 4.1. The schematic electronic arrangement for gamma ray spectrum analysis.

Electronic arrangement consists of a NaI(Tl) scintillation detector, photomultiplier tube (P.M.), preamplifier (Pre.A.), high voltage power supply (H.V), amplifier (Amp.), single-channel-analyzer (S.C.A), counter and timer. Scintillation crystal particularly NaI(Tl) crystal have become the most

popular sensors for detecting gamma radiation. Scintillation detection is primarily useful for pulse measurement, both pulse counting and pulse-height analysis. They are quite efficient in converting absorbed radiation energy into photons of light.

Geometric arrangement has three main components which are source, detector shielding and sample holders. Sample holder is placed between the source and detector. Source shielding has source holder and source collimator which collimates gamma radiation. A good collimator material for high energy gamma radiation is lead. Scintillation detector which is 2"x2" NaI(Tl) is placed into a lead detector holder. The detector shielding prevents it from outside or external radiations. The detector collimators are made of lead and are designed with four different orifices because during the experiment each of the detector collimators can be changed according to the energy of the source. Detector shielding can be moved towards the source according to the desired level of intensity and energy.

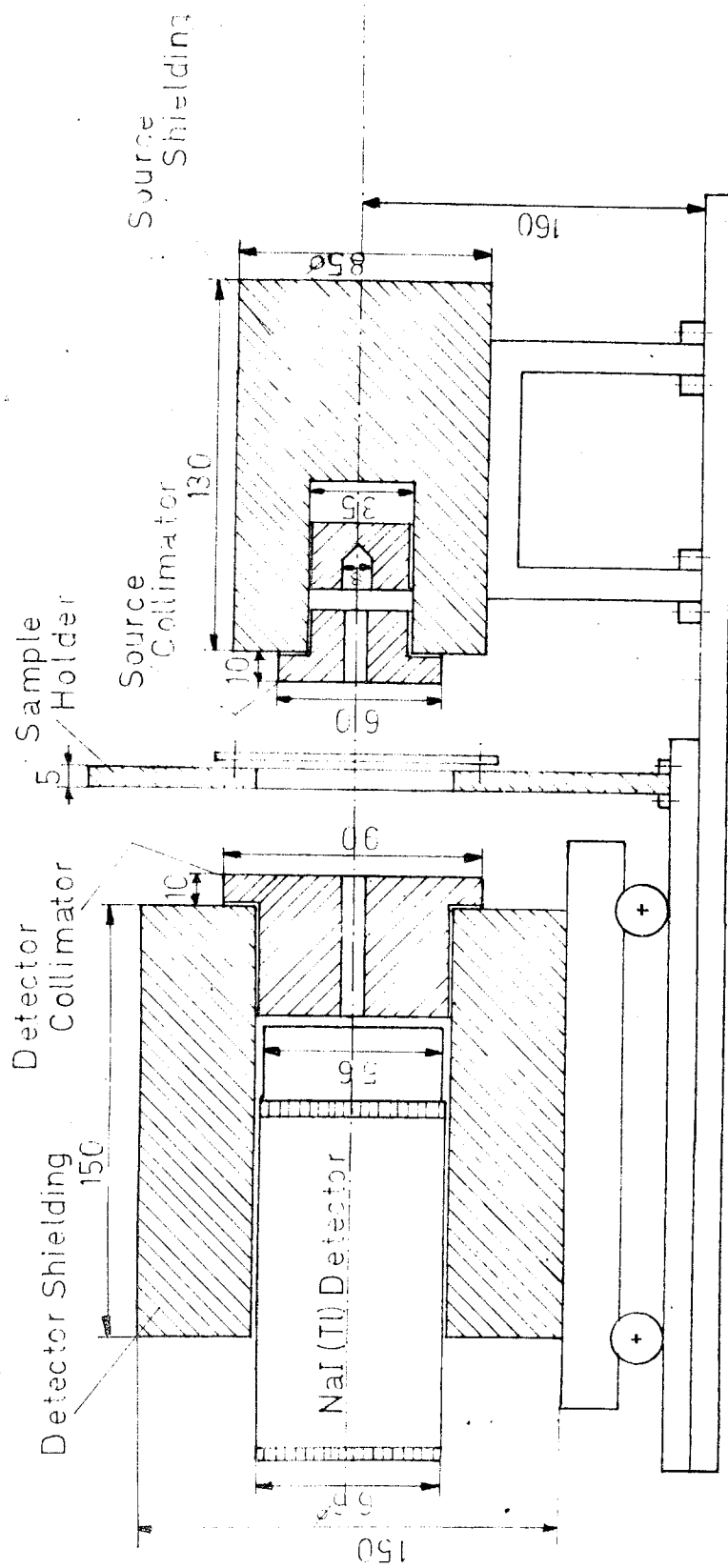


Fig. 4.2 Geometric arrangement of collimation of a source-detector (scale 1:25)



Fig. 4.3 Prototype system for thickness measurements

#### 4.1.2. Calculations of source intensity relative transmission geometry

Radiation from radioisotopes is in general emitted equally in all directions. If a hypothetical sphere of an arbitrary radius  $D$  is constructed around this point source, all the emitted radiation from the source will pass through the spherical surface with equal distribution if no absorption occurs.

This means that the fraction of the total radiation that strikes the detector can be given in terms of the fraction of the spherical surface that is outlined by lines drawn from the point source to the extremities of the detector. This is, by definition, the solid angle subtended by the detector. The fractional solid angle is commonly known as the geometry  $f_G$  of the source-detector arrangement fig. (4.4).

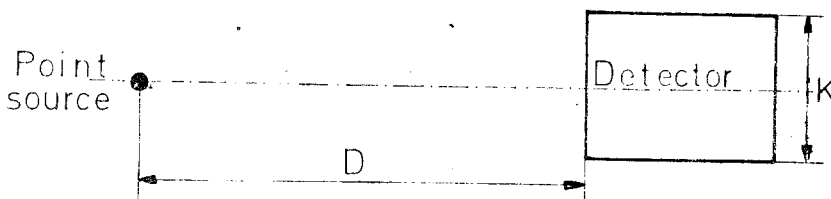


Fig. 4.4. Schematic representation of a point source and cylindrical detector arrangement.

$$\text{Geometry factor } f_G \simeq \frac{A}{4\pi D^2} \quad (4.1)$$

where D is the distance between source and detector,

A is the detector area or collimator orifice area

Which is ( $A = \pi(R/2)^2$ ) and R is the collimator orifice diameter.

Table 4.1. List of source activity

Source	Activity(mci)*	Activity(dis/s)
Am-241	9.894	$3.66 \times 10^8$
Cd-109	2.29	$8.473 \times 10^7$
Pu-238	28.46	$1.05 \times 10^9$

\*One Curie is defined as exactly  $3.7 \times 10^{10}$  (dis/s)

Theoretical intensity whit no absorber:

$$I(0) = A_c \times f_G \times (\text{abundancy \%}) \text{ (photon/s)} \quad (4.2)$$

where  $A_c$  is source activity (dis/s)

According to the system utilized, geometry factor  $f_G$  is:

$$f_G = \frac{\pi(R/2)^2}{4\pi D^2} \quad (4.3)$$

$$f_G = \frac{\pi(5/2)^2}{4\pi(85)^2} \quad 2.162 \times 10^{-4} \quad (4.4)$$

From table 4.2. ,theoretical intensity can be seen for different radioactive sources.



Table 4.2. Theoretical intensity from (Eq. 4.2)

Source	$A_0(\text{dis/s})$	$f_0 \cdot 10^{-4}$	Abundancy	Theo. Inten. (photon/s)
Am-241	$3.66 \times 10^8$	2.16	0.353	27941
Cd-109	$8.47 \times 10^7$	2.16	1	18323
Pu-238	$1.05 \times 10^9$	2.16	0.13	29604

In this calculation, attenuation of air between source and detector and thickness of detector window are neglected.

### 4.1.3. Determination of gamma ray spectrum analysis and energy calibration.

By using the electronic and geometric arrangement illustrated by fig.(4.1) and fig.(4.2) gamma ray spectrum analysis can be performed. The aim of gamma ray spectrum analysis is to establish the energy distribution of the signals at the output of the photomultiplier tube. Before determination of the gamma ray spectrum, study voltage should be determined for a constant threshold voltage and window according to the source in fig.(4.6). After this, gamma ray spectrum is plotted by changing threshold voltage and the following diagram in fig.(4.5) is obtained.

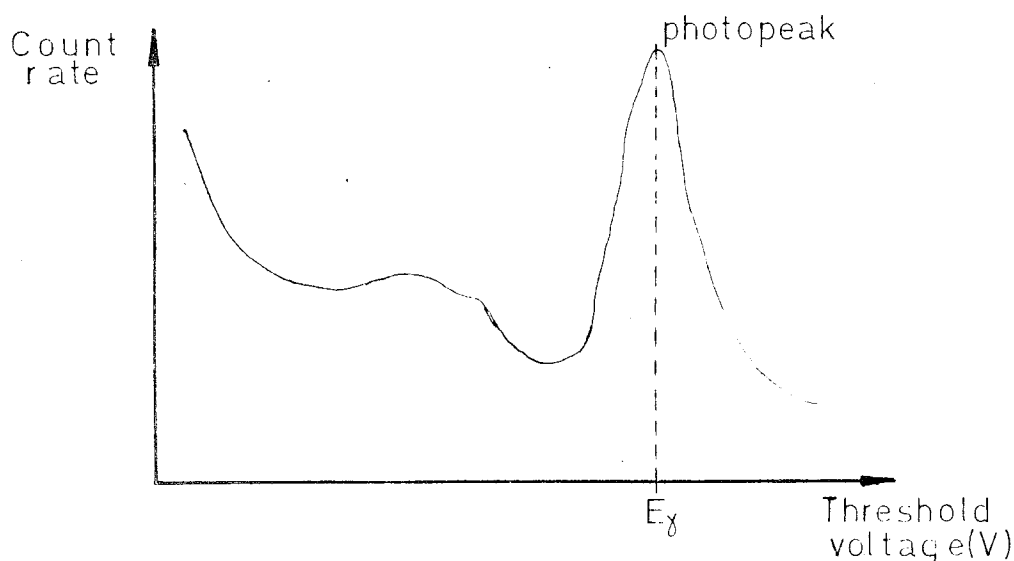


Fig. 4.5. A monoenergetic gamma ray spectrum.

In this diagram, the maximum of the peak corresponds to a gamma photon energy. Ideally this peak should be a vertical line, however, since the multiplication in

the photomultiplier tube and the amplification of the signal in the electronic equipment is not always exactly the same, such a distribution will be observed.

Three gamma ray sources are especially used in this study. They are Am-241, Cd-109, Pu-238.

Table 4.3 Properties of the sources

Source name	Half life	Energy (KeV)	Activity Apr.1984	Abundancy %
Am-241	433yr.	59.543	9.895 mci	35.3
Cd-109	453d.	22-25	2.44 mci	103.3
Pu-238	87.4yr	13.6-22	28.53 mci	13.6

Four detector collimator and source collimators are designed, which have orifice diameters of 3,5,8,10 mm. During the experiment, geometry of the experimental system and the variables of electronic arrangements must always be constant. For this reason, firstly collimator with an orifice diameter of 3mm is placed and the gamma ray spectrum with Am-241 is employed. With the same geometry and high voltage the experiment is repeated for Cd-109 and Pu-238. But the peak of Pu-238 was not detected under the same conditions. In this case, 5mm orifice diameter was placed instead of 3mm one and the distance between source and detector was decreased from 116mm to 85mm. The plot of gamma ray spectrum with Am-241, Cd-109, Pu-238 is illustrated in fig.(4.7), fig.(4.8), fig.(4.9) respectively.

After this procedure, energy calibration curve (source energy vs. threshold voltage) is plotted in fig.(4.10) According to energy calibration curve, full width at half maximum(FWHM) vs. source energy diagram can be plotted in fig.(4.11). According to fig.(4.7),(4.8),(4.9) and table 4.4 can be arranged. Now, the thickness measurement after the calibration of system can be effected.

Table 4.4 Results according to the gamma source used in the experiments

Source name	Threshold voltege(V)	FWHM	HVmax
Am-241	7.51	1.65(V)	598(V)
Cd-109	2.9	1.05(V)	598(V)
Pu-238	2.2	1.00(V)	598(V)

So far, geometry and the system of calibration according to electronic system and radioactive sources has been completed. Now, study voltage, window and threshold voltage and geometry according to radioactive sources can be fixed.

Experimental measurements can now be made and a thickness calibration curve is plotted by using standard "Goodfellow metals" foils illustrated in table 4.5.

Table 4.5 Goodfellow metals

Atomic No.	Metal	No.	Dimensions (mm x mm)	Thickness (mm)
24	Cr	1	100x100	0.002
	Cr	1	100x100	0.005
	Cr	1	100x100	0.01
26	Fe	1	50x50	0.005
	Fe	1	50x50	0.01
	Fe	5	100x100	0.050
29	Cu	1	100x100	0.02
	Cu	1	100x100	0.125
47	Ag	1	100x100	0.025
	Ag	1	100x100	0.125

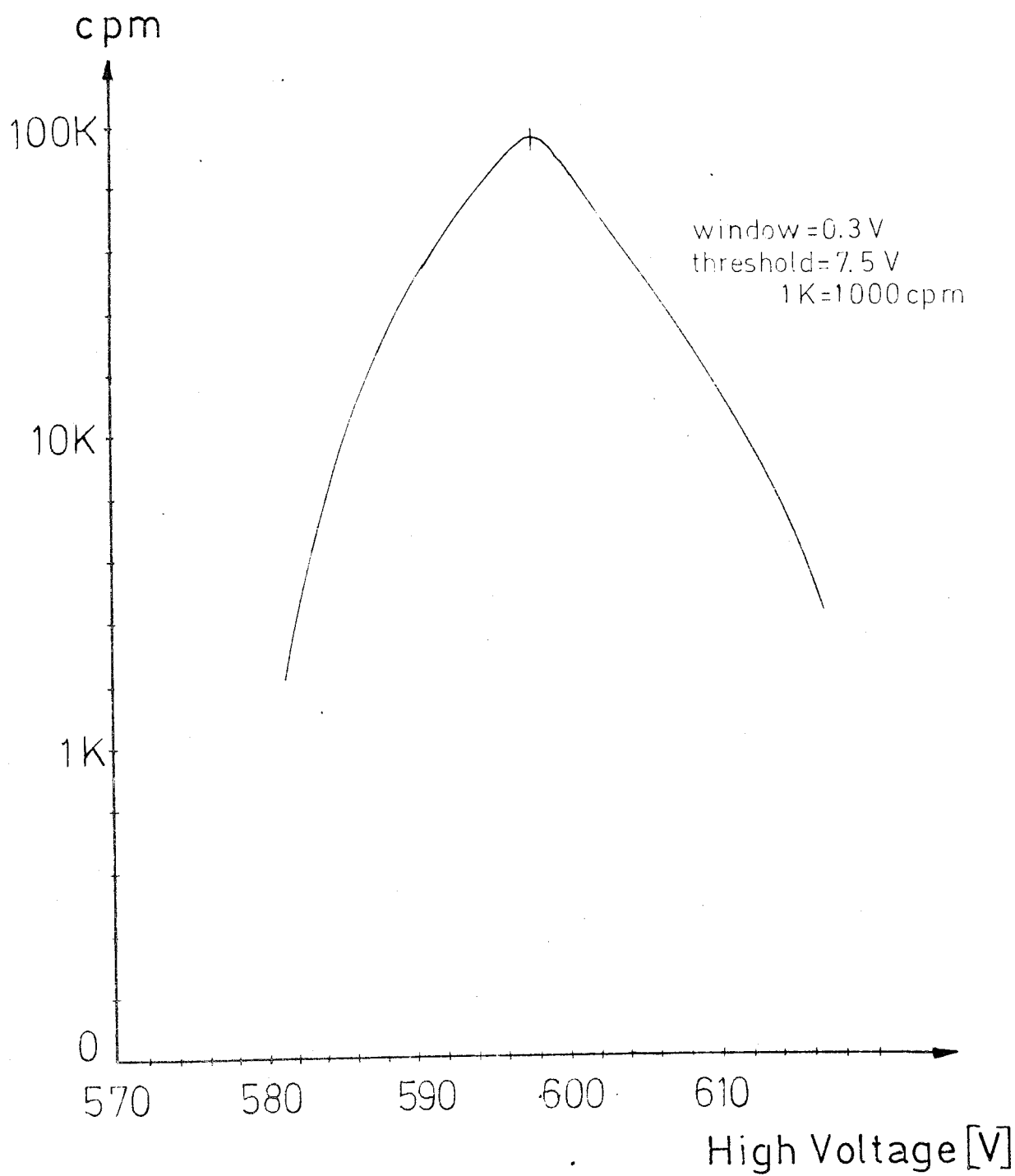


Fig. 4.6 Determination of study voltage

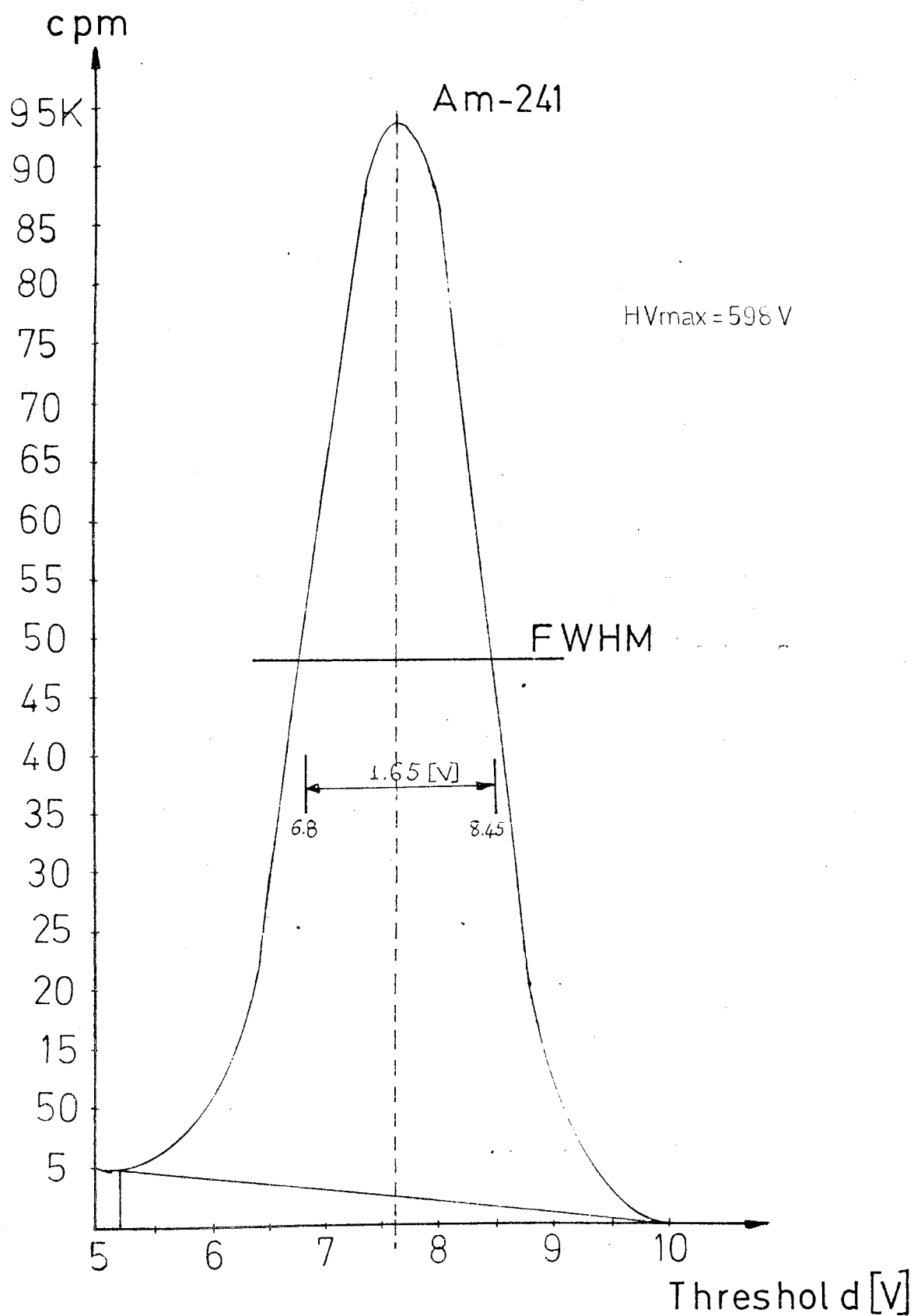


Fig. 4.7 The monoenergetic gamma ray spectrum for Am-241

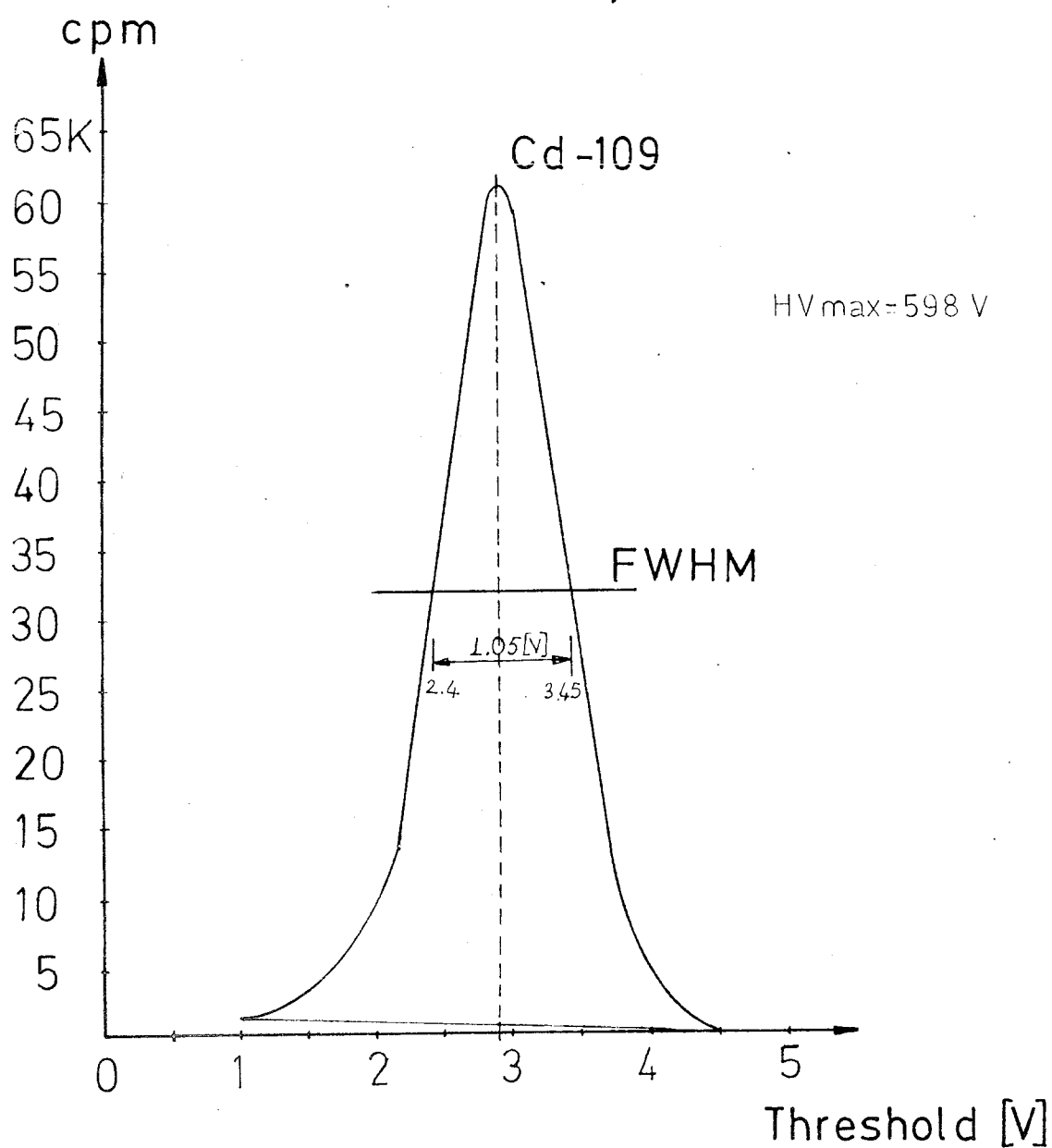


Fig. 4.8 The monoenergetic gamma ray spectrum for Cd-109



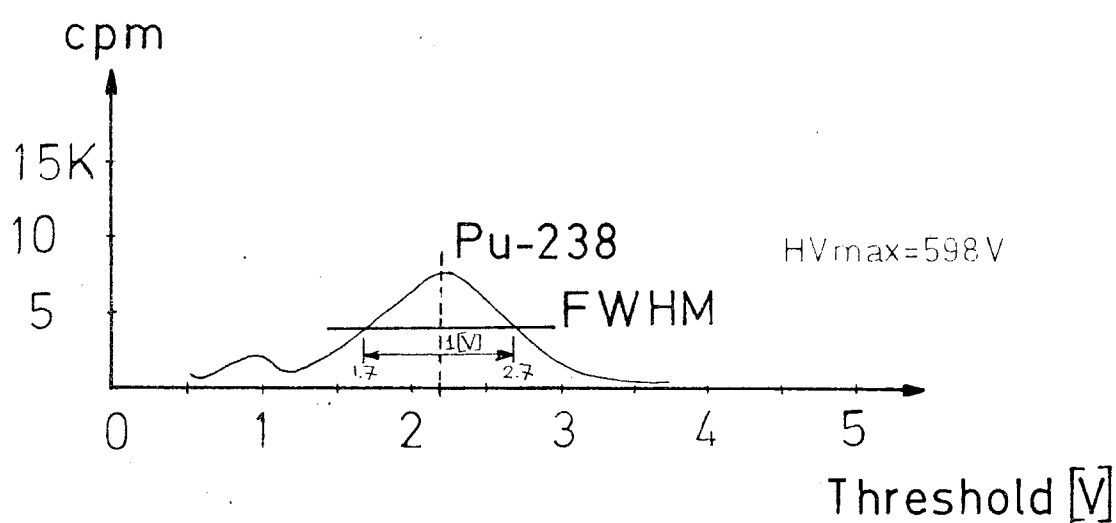


Fig. 4.9 The monoenergetic gamma ray spectrum for Pu-238

Source energy

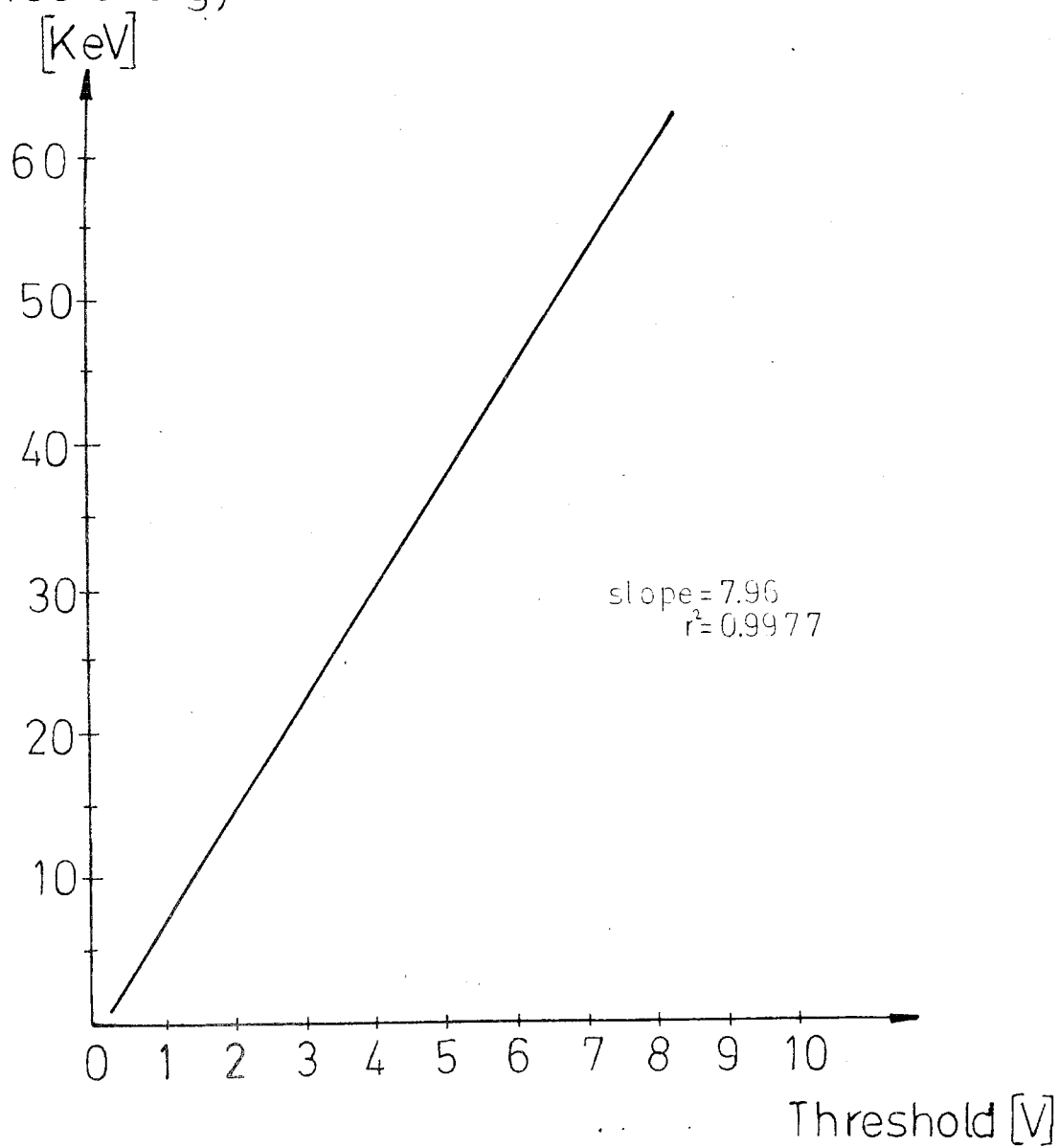


Fig. 4.10 Energy calibration curve

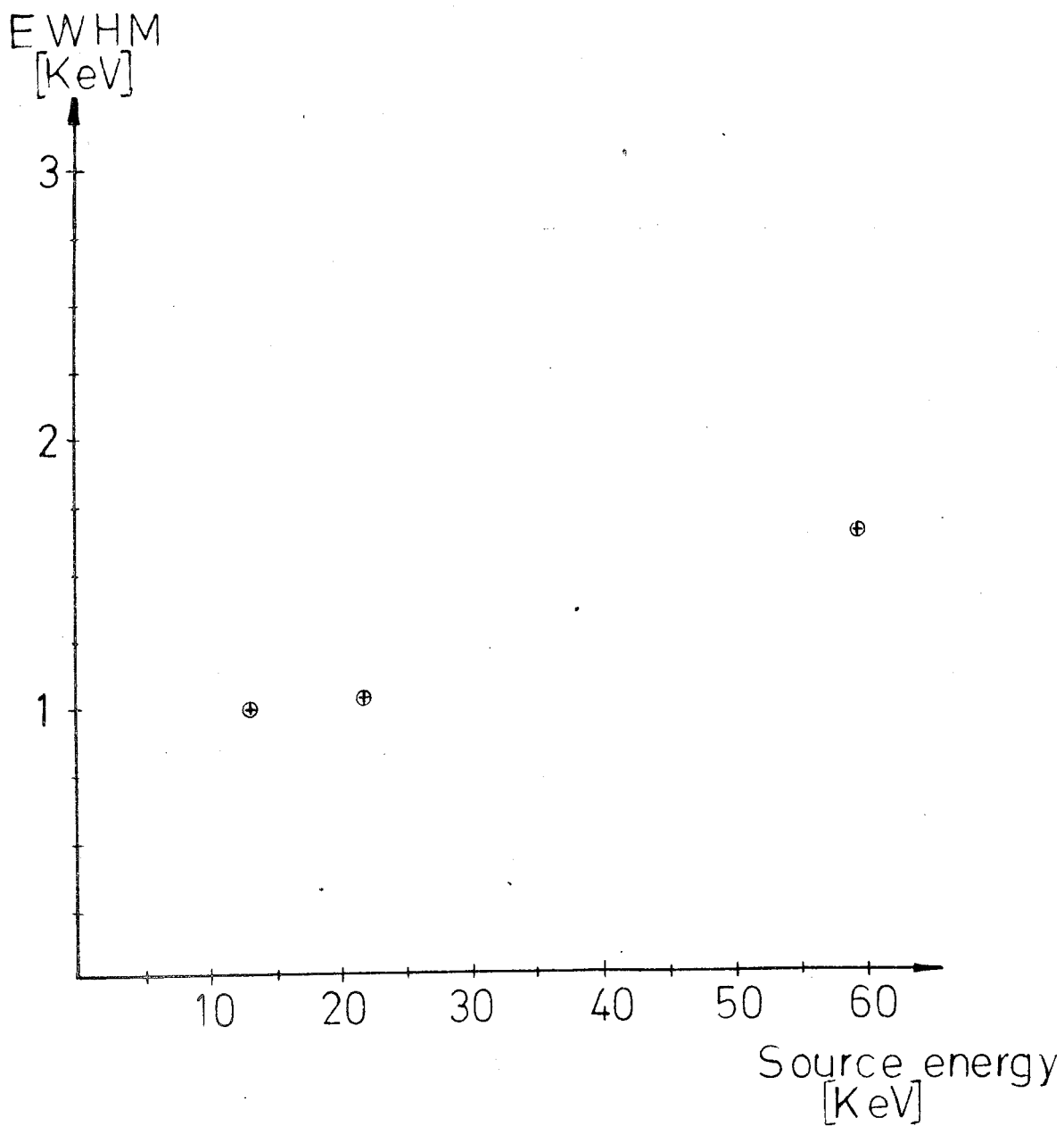


Fig. 4.11 F.W.H.M. vs. source energy

#### 4.1.4. Experimental measurements.

Electronic system according to optimum geometry is calibrated. Then if table 4.6 is studied carefully for each source, thickness measurement can be performed because all the variables are ready. In this case, the thickness calibration curves are plotted because a thickness calibration curve can be used to determine the unknown thickness of a sample. In this experiment, two kinds of thickness calibration curves are prepared. One of them is the theoretical calibration curve and the other is the experimental one. The theoretical and experimental curves are important to compare the experimental and theoretical results.

The experimental results should be close to the theoretical results because the efficiency of the established system can be found by means of these thickness calibration curves. If there is not any difference between the experimental and theoretical results or are not significant, then, it means that the electronic and geometric system had been established properly. The theoretical thickness calibration curve is drawn by means of Eq.(3.1) and  $I(0)$  is found in table 4.2. for the radioactive source, the values of  $\mu$  can be found in table 5.1. or from diagrams of total mass attenuation coefficient vs. source energy (see also APPENDIX A). In Eq.(3.1), the values of  $I(x)$  are calculated by changing the thickness  $x$  and the theoretical thickness calibration curve is plotted versus the thickness. Experimental thickness calibration curve can be

plotted by means of the electronic and geometric arrangement. For example, using the radioactive source Am-241 and sample Ag, the electronic and geometric arrangement for the experiment, is performed as follows: From table 4.6. and fig.(4.7), the high voltage, threshold and window are 598 (V), 5.25(V), 4.6(V) respectively, for the source Am-241.

Distance between source and detector is adjusted to 85mm and 5mm collimator orifice diameter is placed into the detector shielding.

Table 4.6 Experimental results with  
radioactive sources.

Variables	Radioactive sources		
	Am-241	Cd-109	Pu-238
HVmax (V)	598	598	598
Threshold (V)	5.25	1	1.2
Window (V)	4.6	3.6	2.3
Distance (mm) (source-detector)	85	85	85
Collimator orifice diameter (mm)	5	5	5
Experimental intensity(Counts/s)	17279	8180	1123

Then, all the variables are set for the source Am-241 to count measurements. After this, a standard foil, for example, silver of 25( $\mu$ m) is placed in sample holder

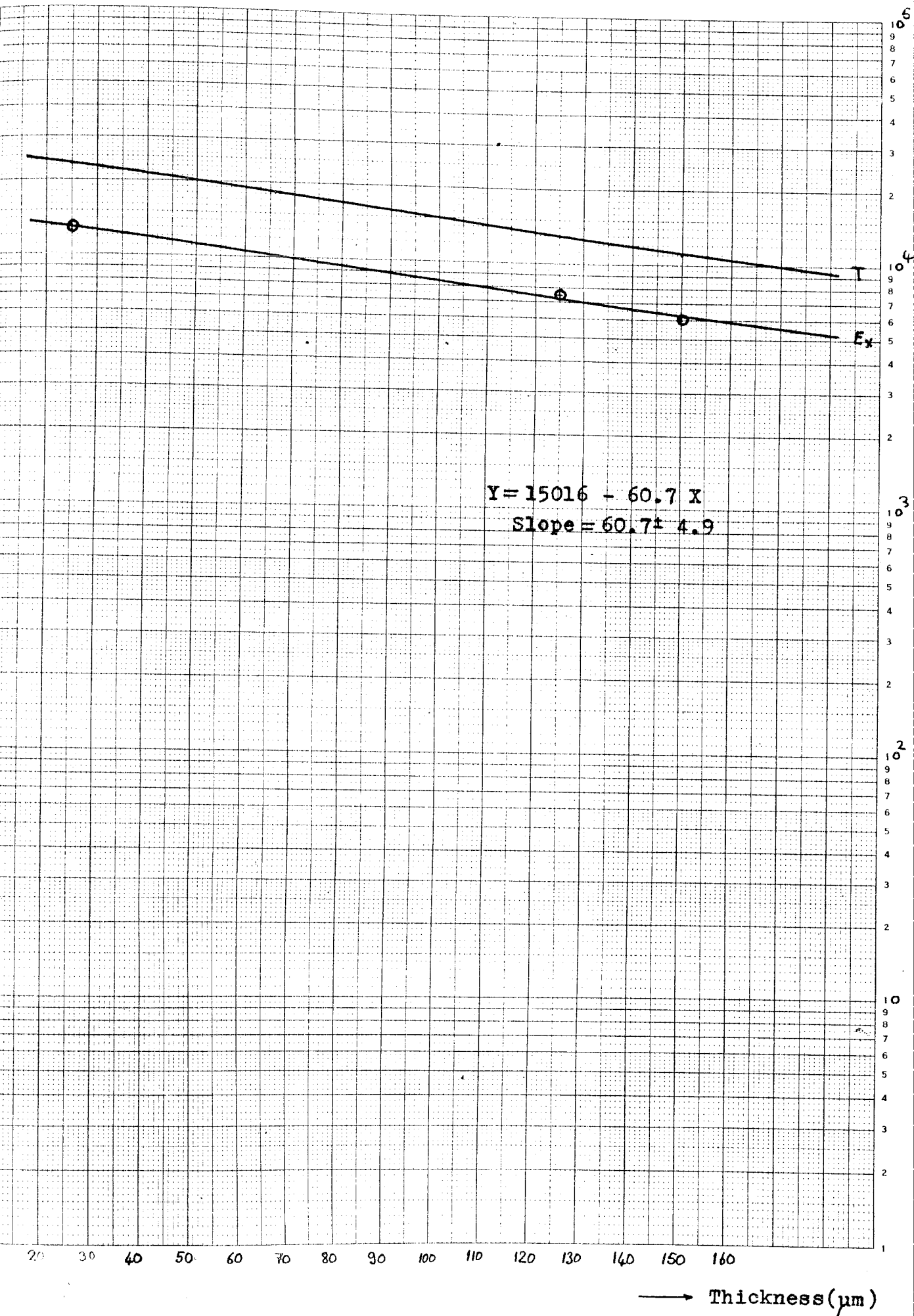
and then the existing count is 13500 counts per second  $I(x)$ . The same way, other standard foil thicknesses are used and a lot of experimental points can be found. So the experimental calibration curve can be plotted. The most satisfactory experiment amongst the three sources used was with the source Cd-109. The slope of its calibration curves were suitable for the measurements. The sensitivity of an instrument is often defined as the change in the response for a given change in the variable being measured. For example, the sensitivity for the radiogauge would be written as

$$S = \frac{\partial I(x)}{\partial x} \quad (\text{counts/thickness}) \quad (4.5)$$

Thus the sensitivity is just the slope of the calibration curve (Ga-67). The sensitivity vary with  $x$ . If the change of intensity according to change in the thickness is significant the slope of the calibration curve is significant and the measuring sensitivity of the instrument is suitable for the measurements.

The experimental calibration curves are helpful in finding any unknown thickness desired. For example, if a thickness of sample is unknown, as explained before that sample is placed in the sample holder and a count is observed from counter and with the help of the count from the experimental thickness calibration curve, the unknown thickness can be found.

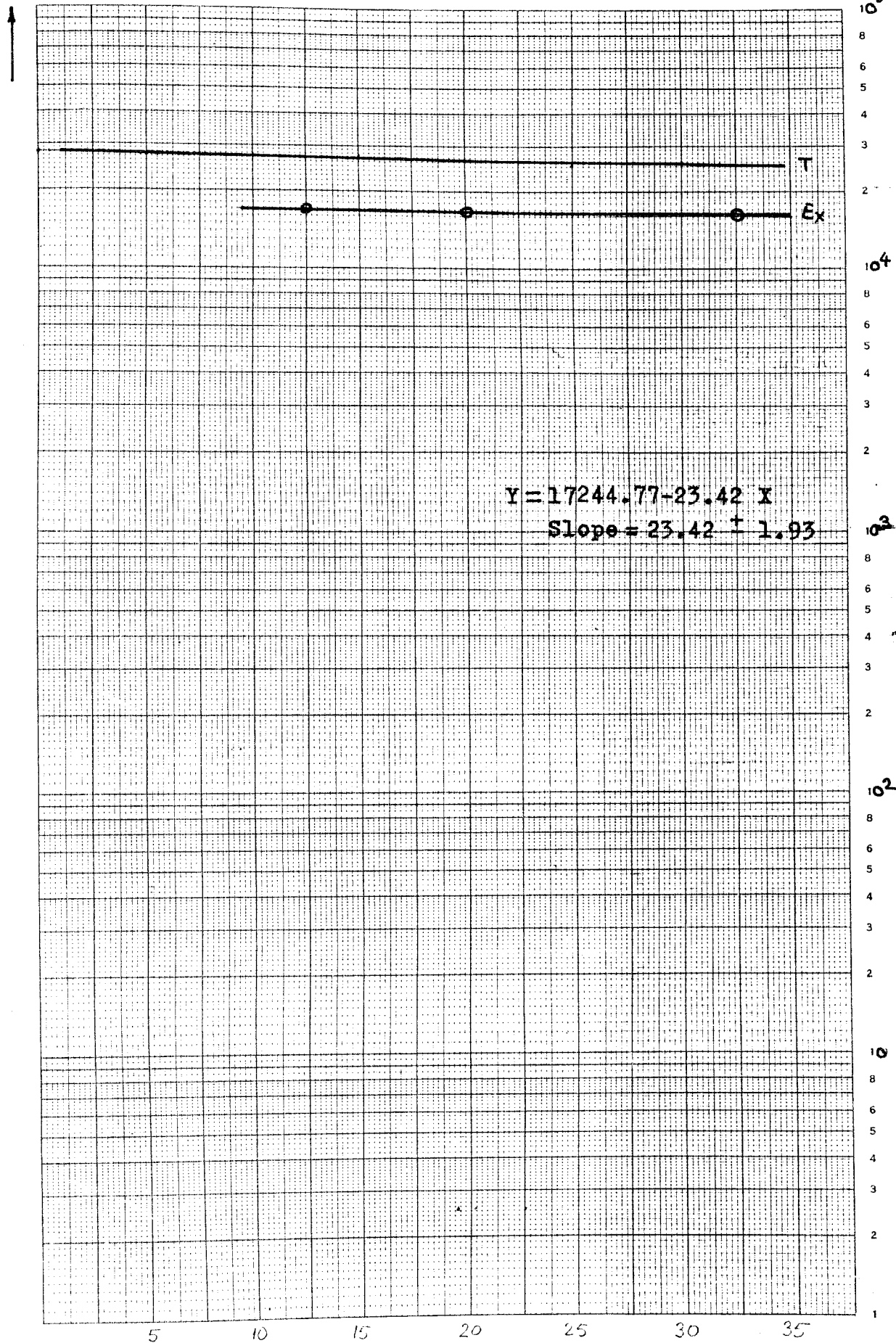
Fig. 4.12 THEORETICAL AND EXPERIMENTAL THICKNESS  
CALIBRATION CURVES FOR RADIOACTIVE  
SOURCES:Am-241,Cd-109,Pu-238  
(Logarithmic scale)





Sample Cu

cps



Thickness (μm)

Source Am-241

Sample Fe

cps



$10^4$

8

6

5

4

3

2

$10^3$

8

6

5

4

3

2

$10^2$

8

6

5

4

3

2

$10^1$

8

6

5

4

3

2

$10^0$

8

6

5

4

3

2

1

5 10 15 20 25 30 35 40 45 50 55 60



Thickness ( $\mu\text{m}$ )

Source Am-241

Sample Cr

cps



$10^6$

8

6

5

4

3

2

$10^4$

8

6

5

4

3

2

$10^3$

8

6

5

4

3

2

$10^2$

8

6

5

4

3

2

$10^1$

8

6

5

4

3

2

$10^0$

8

6

5

4

3

2

1

$$Y = 17157.2 - 10X$$

$$\text{Slope} = 10 \pm 3.26$$

1 2 3 4 5 6 7 8 9 10

→ Thickness ( $\mu\text{m}$ )

Source Cd-109

Sample Ag

cps

$10^5$

8

6

5

4

3

2

$10^4$

8

6

5

4

3

2

$10^3$

8

6

5

4

3

2

$10^2$

8

6

5

4

3

2

$10^0$

8

6

5

4

3

2

1

$$Y = 6505.51 - 38.49 X$$

$$\text{Slope} = 38.49 \pm 2.35$$

T

E<sub>x</sub>

→ Thickness (μm)

Source Cu-109  
Sample Cu

cps



$10^5$

8

6

5

4

3

2

$10^4$

8

6

5

4

3

2

$10^3$

8

6

5

4

3

2

$10^2$

8

6

5

4

3

2

10

8

6

5

4

3

2

1

$$Y = 7473.8 - 107.7 X$$

$$\text{Slope} = 107.7 \pm 1.79$$

Thickness ( $\mu\text{m}$ )

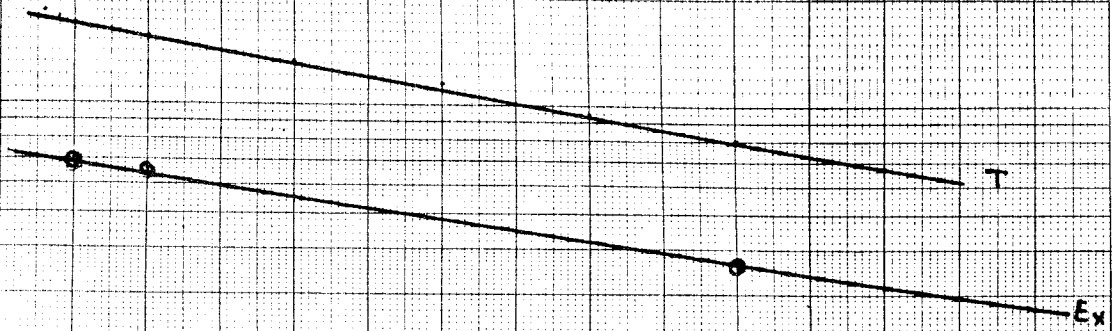
Source Cd-109

Sample Fe

cps



10<sup>6</sup>  
8  
6  
5  
4  
3  
2  
  
10<sup>4</sup>  
8  
6  
5  
4  
3  
2  
  
10<sup>3</sup>  
8  
6  
5  
4  
3  
2  
  
10<sup>2</sup>  
8  
6  
5  
4  
3  
2  
  
10  
8  
6  
5  
4  
3  
2  
  
1



$$Y = 7320.5 - 73.26 X$$
$$\text{Slope} = 73.26 \pm 1.17$$

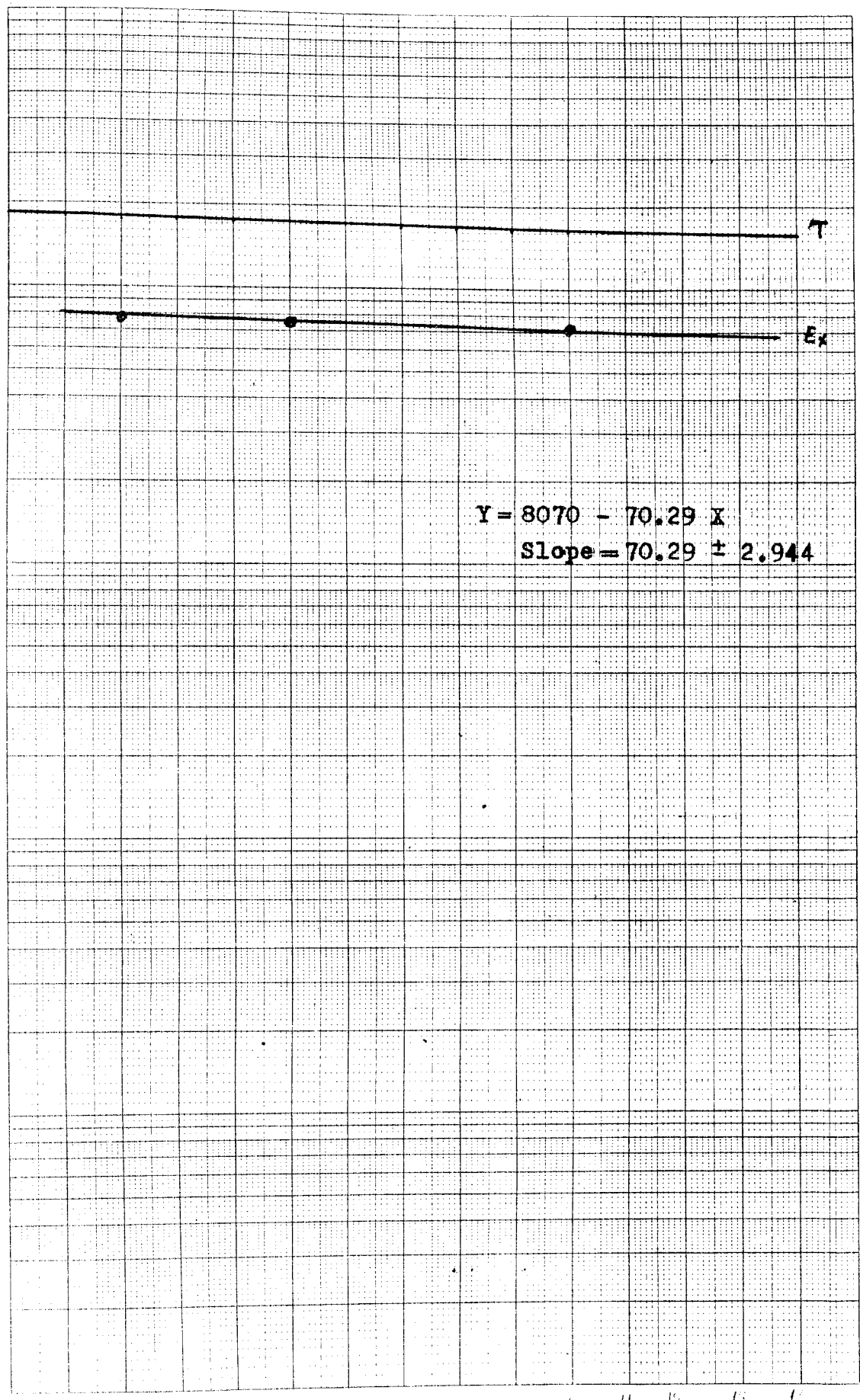
→ Thickness (μm)



Source Cd-109

Sample Cr

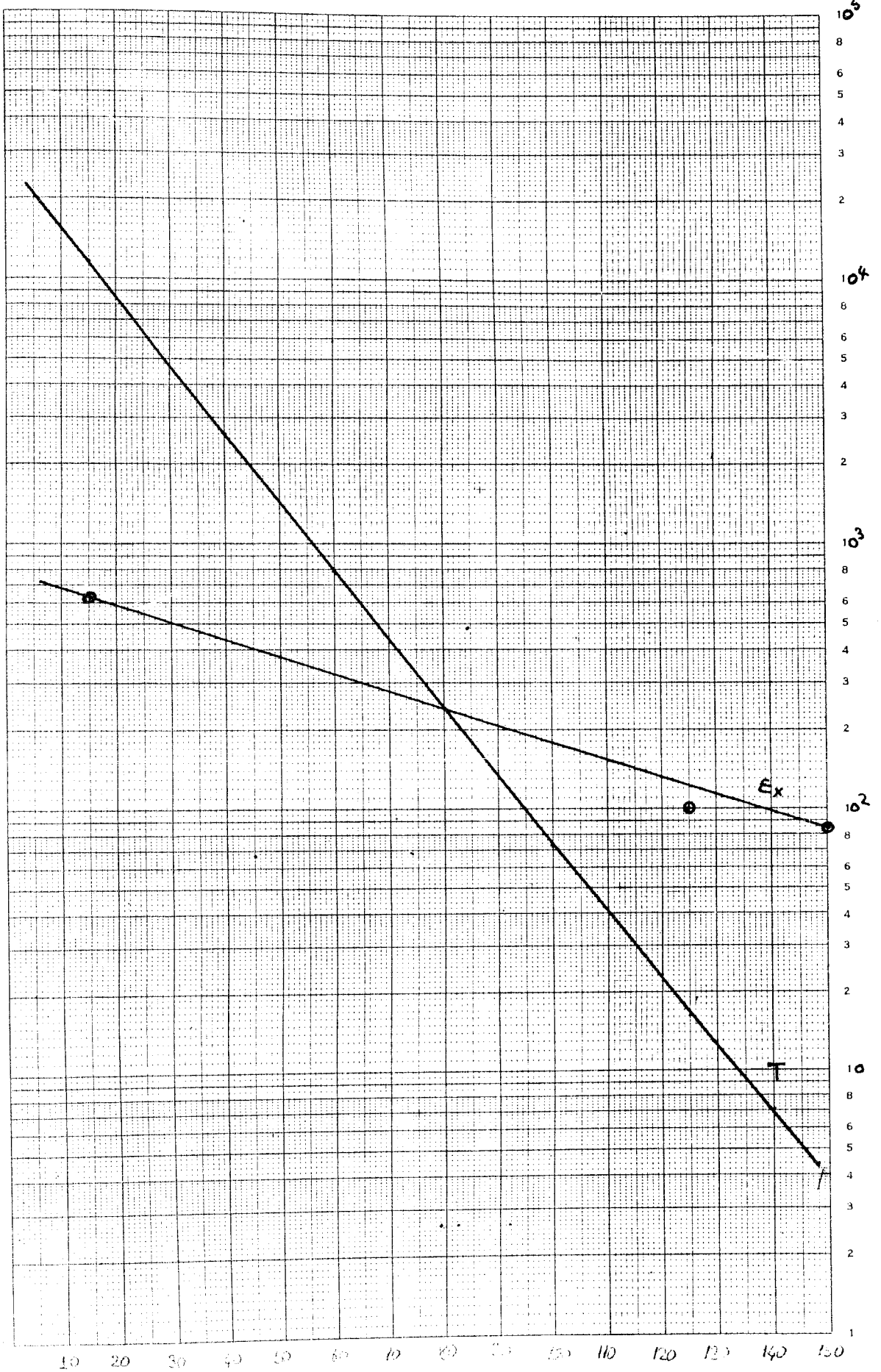
cps



→ Thickness ( $\mu\text{m}$ )

Source Pu-238  
Sample Ag

cps  
↑



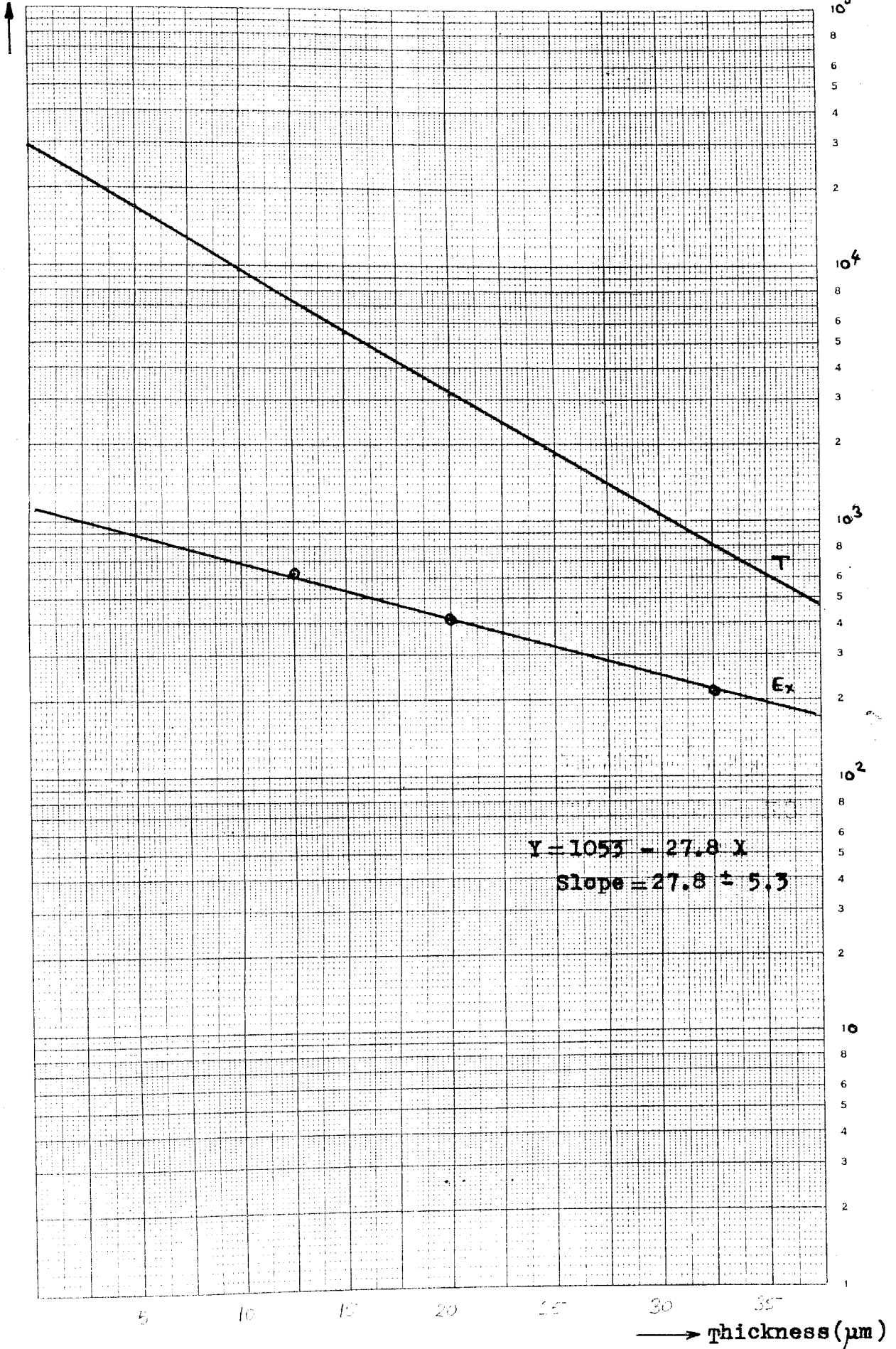
→ Thickness ( $\mu\text{m}$ )



Source Pu-238

Sample Cu

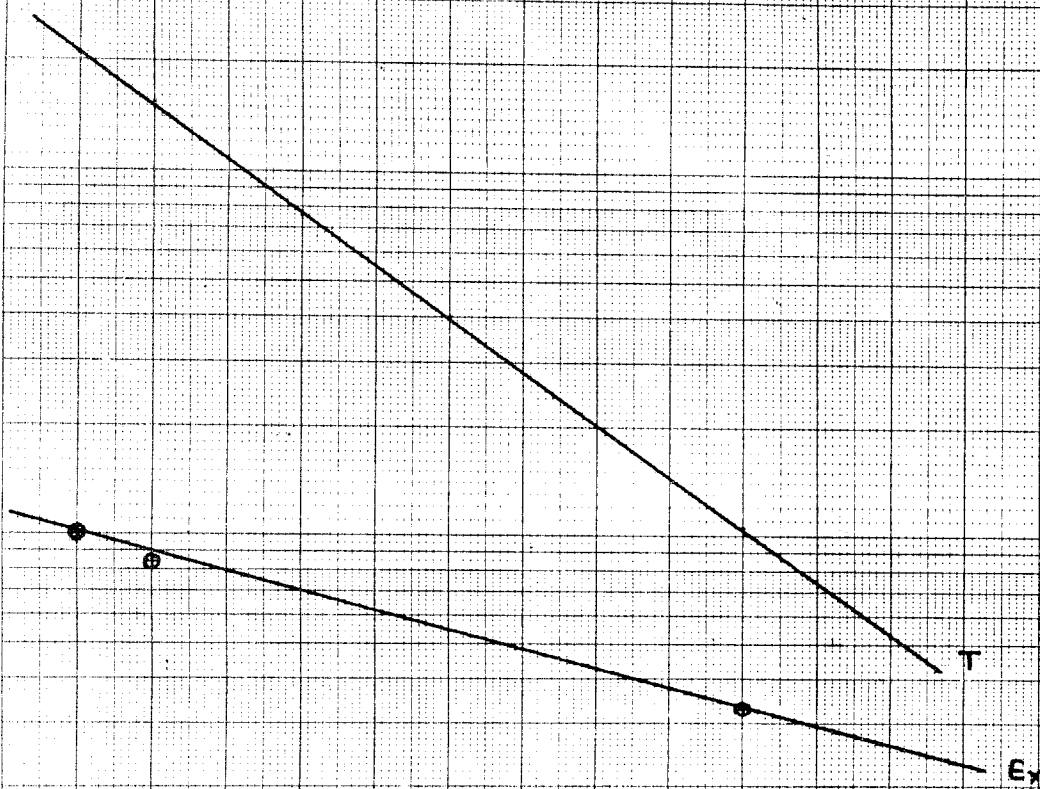
cps



cps



1  
8  
6  
5  
4  
3  
2  
  
10<sup>5</sup>  
8  
6  
5  
4  
3  
2  
  
10<sup>4</sup>  
8  
6  
5  
4  
3  
2  
  
10<sup>3</sup>  
8  
6  
5  
4  
3  
2  
  
10<sup>2</sup>  
8  
6  
5  
4  
3  
2  
1

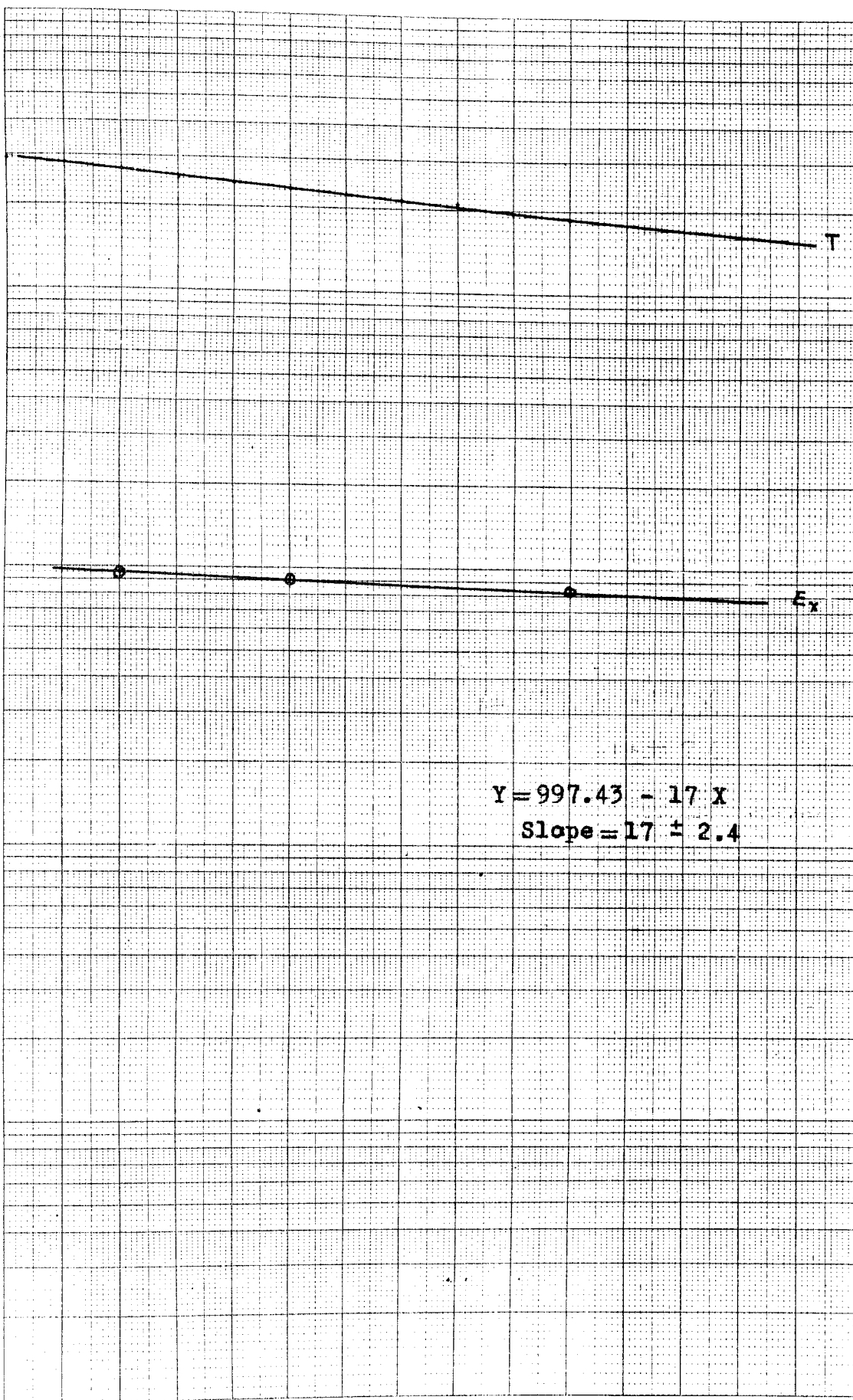


→ Thickness (μm)

cps



10<sup>5</sup>  
8  
6  
5  
4  
3  
2  
  
10<sup>4</sup>  
8  
6  
5  
4  
3  
2  
  
10<sup>3</sup>  
8  
6  
5  
4  
3  
2  
  
10<sup>2</sup>  
8  
6  
5  
4  
3  
2  
  
10  
8  
6  
5  
4  
3  
2  
1



→ Thickness (μm)

## V. MINIMUM DETECTION LIMITS

Evaluation of minimum detection limit is required for each source and sample because this determines the measuring ability of calibrated system. There is not an exact rule for the calculation of minimum detection limits and requires some assumptions to be made, for example, from equation

$$I(x) = I(0) e^{-\mu_p x} \quad (5.1)$$

If  $\sigma(I(0))$  is error of counting rate with no sample and if difference between the counting rate with no sample and the counting rate with sample is greater than  $\sigma(I(0))$ , namely,  $\sigma(I(0)) < I(0) - I(x)$ , this indicates that there is a sample which has at least the minimum thickness between the source and detector.

Now, an assumption can be done for the difference between  $I(0)$  and  $I(x)$ . So, it can be that

$$I(x) = I(0) - 2 \sigma(I(0)) \quad (5.2)$$

where  $\sigma(I(0))$  is the standard deviation of the counting rate with no sample and equals to  $\sqrt{I(0)}$  and previous equation is

$$I(x) = I(0) - 2\sqrt{I(0)} \quad (5.3)$$

In this case, when the difference between  $I(0)$  and  $I(x)$  equals to two standard deviations of the counting rate with no sample, there is a sample which will be measured the thickness. From Eq.(5.1), thickness  $x$  can be solved:

$$x = \frac{1}{\mu\rho} \ln \frac{I(0)}{I(x)} \quad (5.4)$$

and if  $I(x) = I(0) - 2\sqrt{I(0)}$  then (5.5)

$$x_{min} = \frac{1}{-\mu\rho} \ln \left( \frac{1}{1 - \frac{2}{\sqrt{I(0)}}} \right) \quad (5.6)$$

Table 5.1 Minimum detection limits( $\mu m$ )

Source	Samples			
	Cr	Fe	Cu	Ag
Am-241	21.32	15.83	10.69	2.52
Cd-109	1.83	1.35	0.71	1.5
Pu-238	1.33	0.92	0.54	1.01

Table 5.2 Total mass attenuation coefficient for sources and samples ( $\text{cm}^2/\text{g}$ ).

Samples		Am-241	Cd-109	Pu-238
	Density( $\text{g}/\text{cm}^3$ )	59.6(KeV)	22.2(KeV)	13.6(KeV)
Magnesium	1.74	0.26	1.89	6.2
Aluminum	2.699	0.3	2.5	11.0
Zinc	6.5	1.74	30.0	110.0
Crom	7.19	1.00	17.0	64.0
Mangenese	7.43	1.1	16.0	60.0
Iron	7.87	1.23	21.0	85.0
Cadmium	8.65	6.3	15.0	64.0
Nickel	8.9	1.55	26.0	110.0
Copper	8.96	1.6	35.0	125.0
Silver	10.49	5.8	14.18	58.0

For the calculation of minimum detection limits every the radioactive sources and samples, with the help of the table (4.6) and table (5.2) the minimum detection limits can be calculated for each sample and the source such as table (5.1).

If the table (5.1) is studied, for example, the minimum detection limit is  $2.52(\mu\text{m})$  for the radioactive source Am-241 and sample silver. In other words, one can measure or detect a thickness of any sample until thickness of  $2.52(\mu\text{m})$  for silver with the source Am-241.

## VI. DISCUSSION AND CONCLUSION

The aim of this study was to develop a thickness gauge to measure the thickness of thin foils in microns. A thickness gauge can be effected at the end of this study and the thickness calibration curves were prepared to find the unknown thickness of samples. In this experiment, measurement is non-destructive and no contact is required with the material being measured. Such instruments are therefore used on continuously produced material travelling at high speed or at high temperature, on soft or malleable materials and on those where the surface finish is important.

The first task to be accomplished before starting with the experiments is the choice of the source. The above mentioned equation  $\mu x = 2$  is to be used in order to find the optimum source.

Low energy sources should be chosen since the thickness measurements to be performed are of the order of microns according to the equation  $\mu x = 2$ . Low energy photons (5.89 KeV of the source of Fe-55) are absorbed within the detector window thickness and therefore the count rate obtained will be low. Therefore, the thickness of materials such as the samples Al, Mg could not be measured. The experiments with the source Am-241 and the sample Ag is suitable but the calibration curves obtained

for the samples Cr, Fe and Cu are not satisfactory due to the attenuation in materials that are less dense than the sample Ag is weak since the energy of radioactive source Am-241 is high.

There are other problems about the calibration curves, too. For example, the experimental calibration curves of experiments with the source Pu-238 intersect the theoretical ones, in which case the results of the experiment are invalid. The experimental with the sample Ag can be given as an example:

The energy of the source Pu-238 ranges from 13.6 to 22 KeV. The K-edge is absorbed about 25.517 KeV in the graph of total mass attenuation coefficient vs. source energy prepared for the sample Ag (see also APPENDIX A). This is close to the max energy of the source Pu-238 and the region where the total mass attenuation coefficient changes sharply. This is due to excitation of the sample Ag by the source Pu-238 and the successive de-excitation thereby releasing the energy acquired in the form of electromagnetic energy which, in turn, results in a higher count rate. Hence, the experimental and theoretical calibration curves intersect each other as can be seen in the plot and this is an unexpectedly erroneous situation. In addition, the experimental and theoretical calibration curves of the source Cd-109 are parallel and the energy of the source Cd-109 for the samples used had been selected properly and the experimental calibration curves are suitable to measure the thickness of samples.



The alignment of the axes of the collimators are as shown in fig.(4.2) must be assured, otherwise the collimator orifices will not face each other exactly in which case insufficient and erroneous counts will be obtained. That the detector is removable is of great use since it allows for easy adjustment of detector-to-source distance depending upon the energy and intensity of the source. The number of photons incident on unit area decreases as the distance from source to detector increases (From Eq.(4.1)) and the number of photons incident on the detector should be large so that the error coming from counts is small. The error can be expressed as the relative standard deviation that is

$$\frac{\sigma(n)}{n} = \frac{\sqrt{n}}{n} = \frac{1}{\sqrt{n}} \quad (6.1)$$

where n is total counts (Gr-67)

As can be seen from this equation, if counts are large the relative standard deviation is small.

As explained before according to the radioactive sources and the samples, the thickness gauge has been adjusted. In the experiment, if the thickness of materials of high density is measured by the high energy source, the better results can be obtained but for the source selection of the foil thickness, the energy of source should not correspond to the K-edge region.

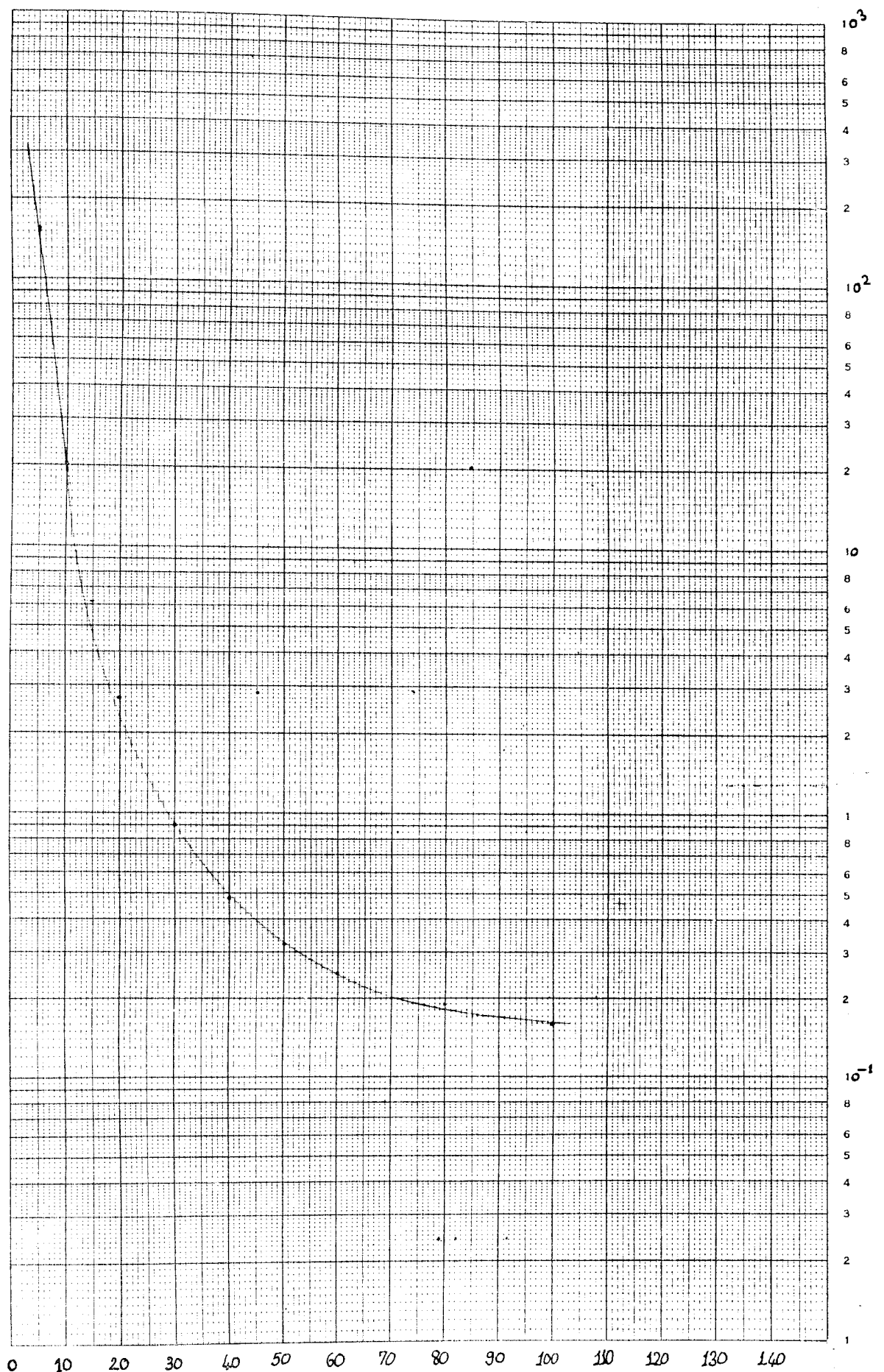
For each sources and samples, the minimum detection limits had been found and users have an idea about the minimum detection limits. In this study, the most satisfactory results amongst the three sources were obtained with the source Cd-109 and partly the source Am-241. But the source Pu-238 can be used to measure the thickness in the experiments if the optimum samples are selected according to the equation  $\mu x = 2$  but it is on condition that the region of K-edge is taken into consideration.

APPENDIX A

TOTAL MASS ATTENUATION COEFFICIENT (T.M.A.C.)  $\text{[cm}^2/\text{g]}$

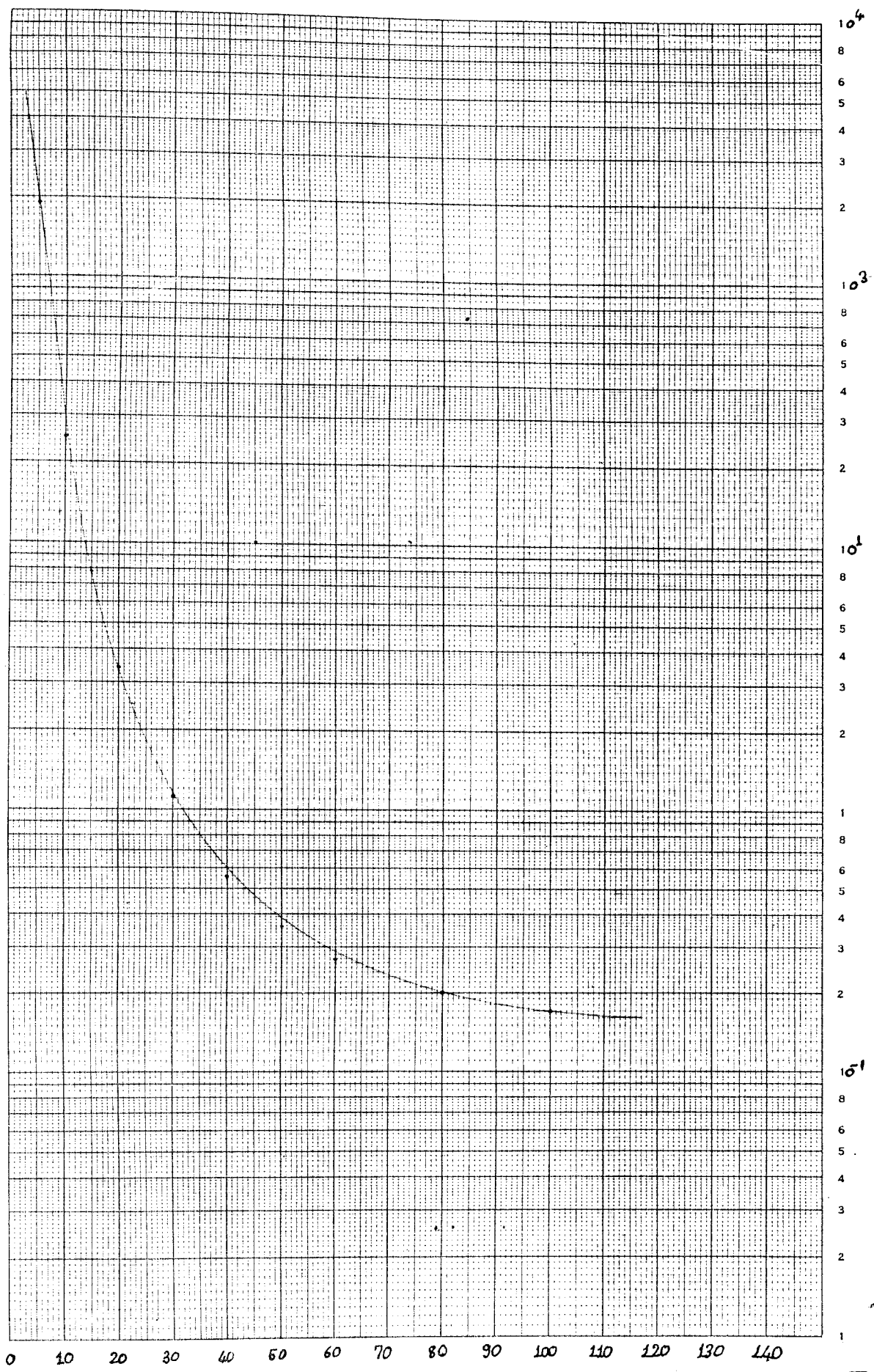
VS. RADIOACTIVE SOURCE ENERGY (E)  $\text{[KeV]}$  DIAGRAMS.  
(Logarithmic scale)

I.M.A.C. for Mg



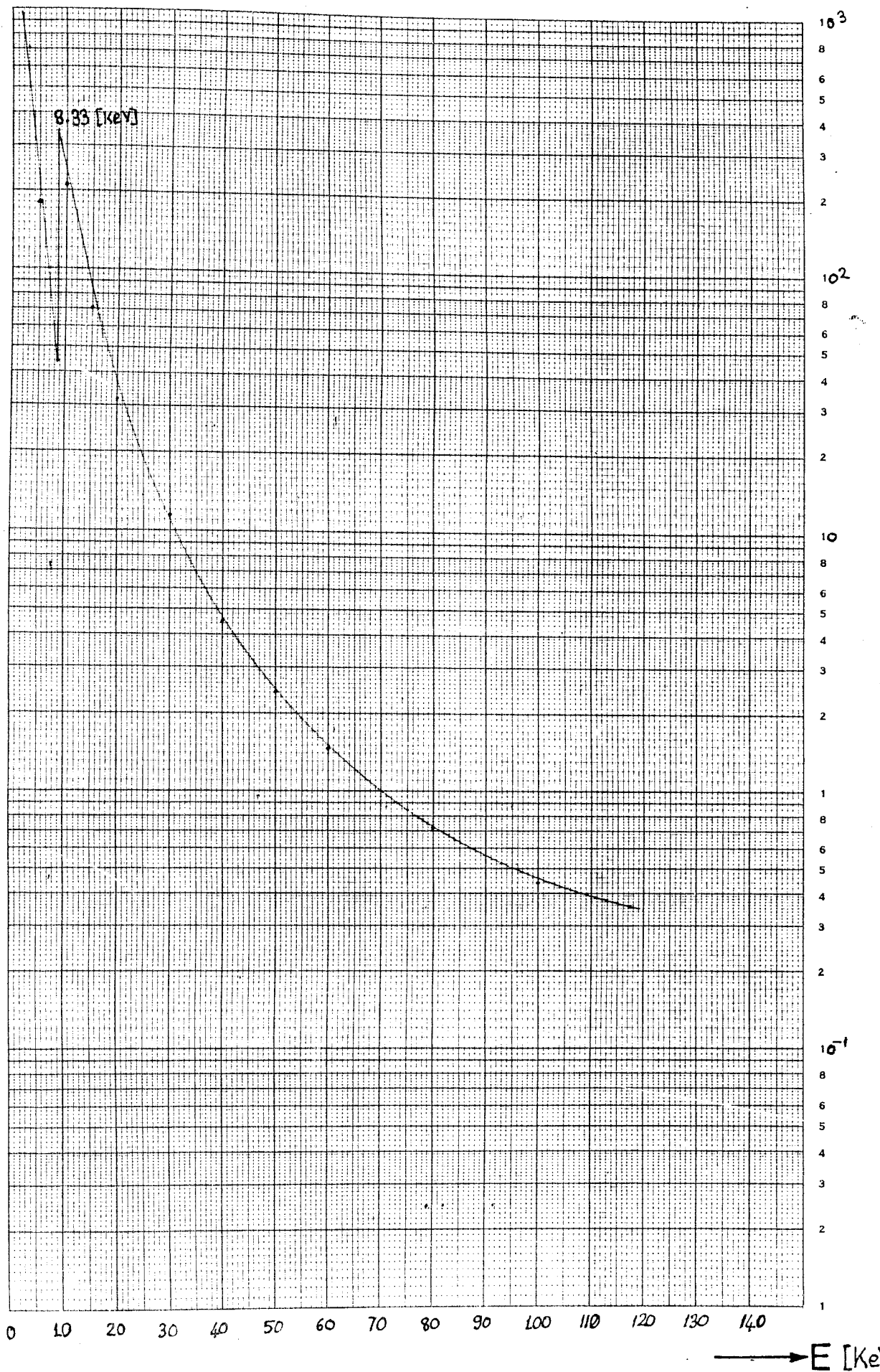
→ E

I.M.A.C. for Al

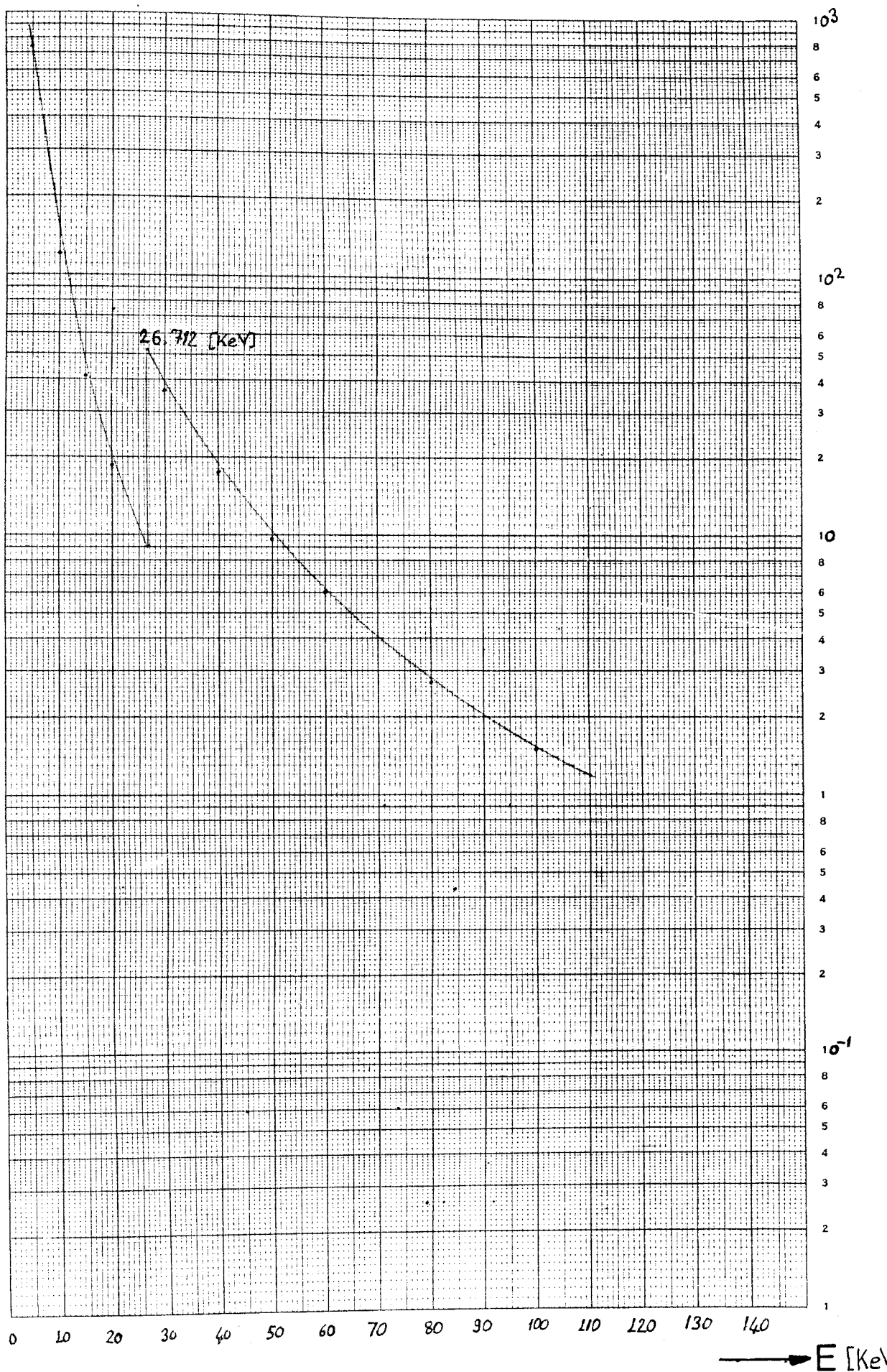


→ E

T.M.A.C. for Ni

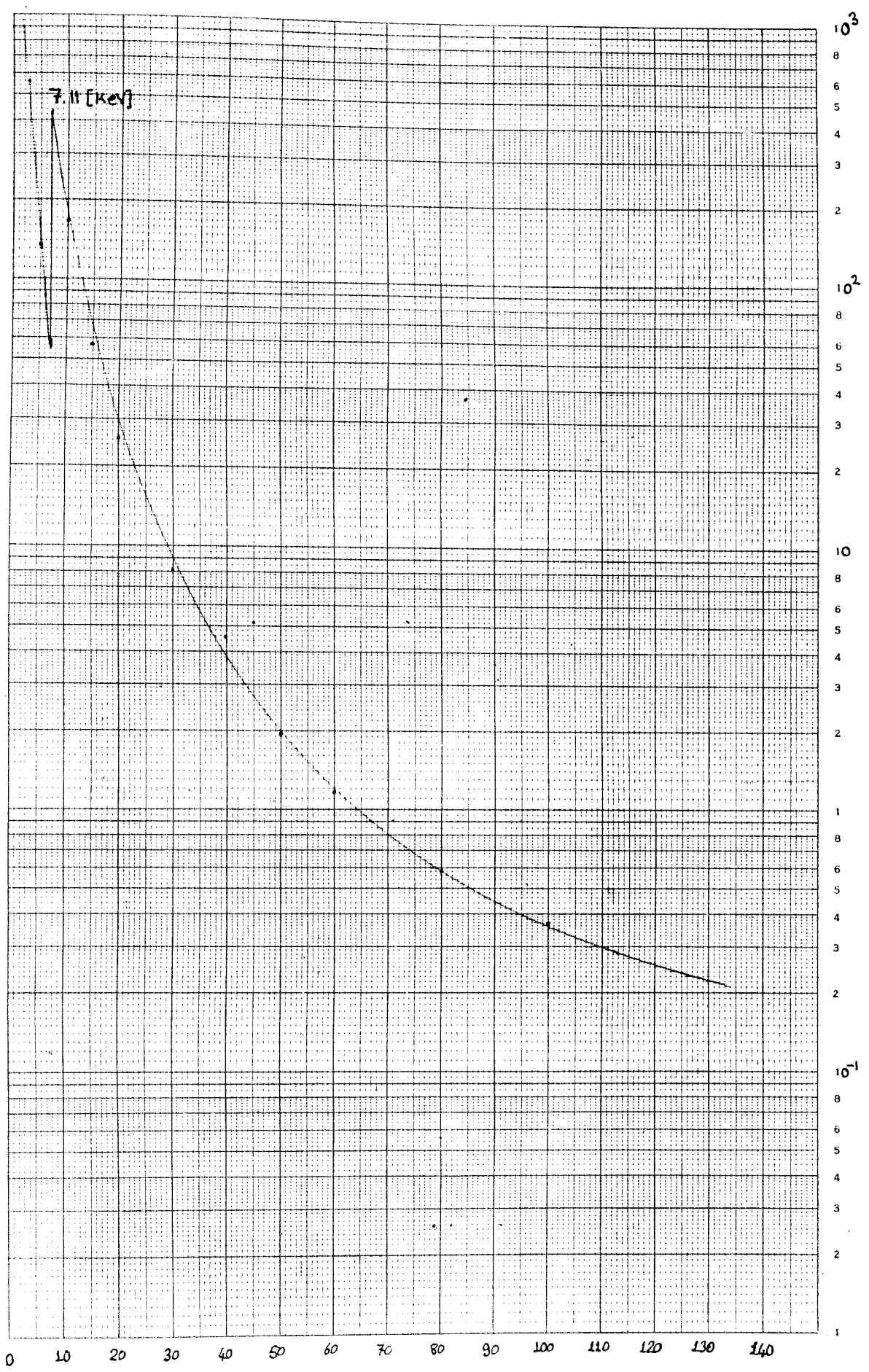


M.A.C. for Cd





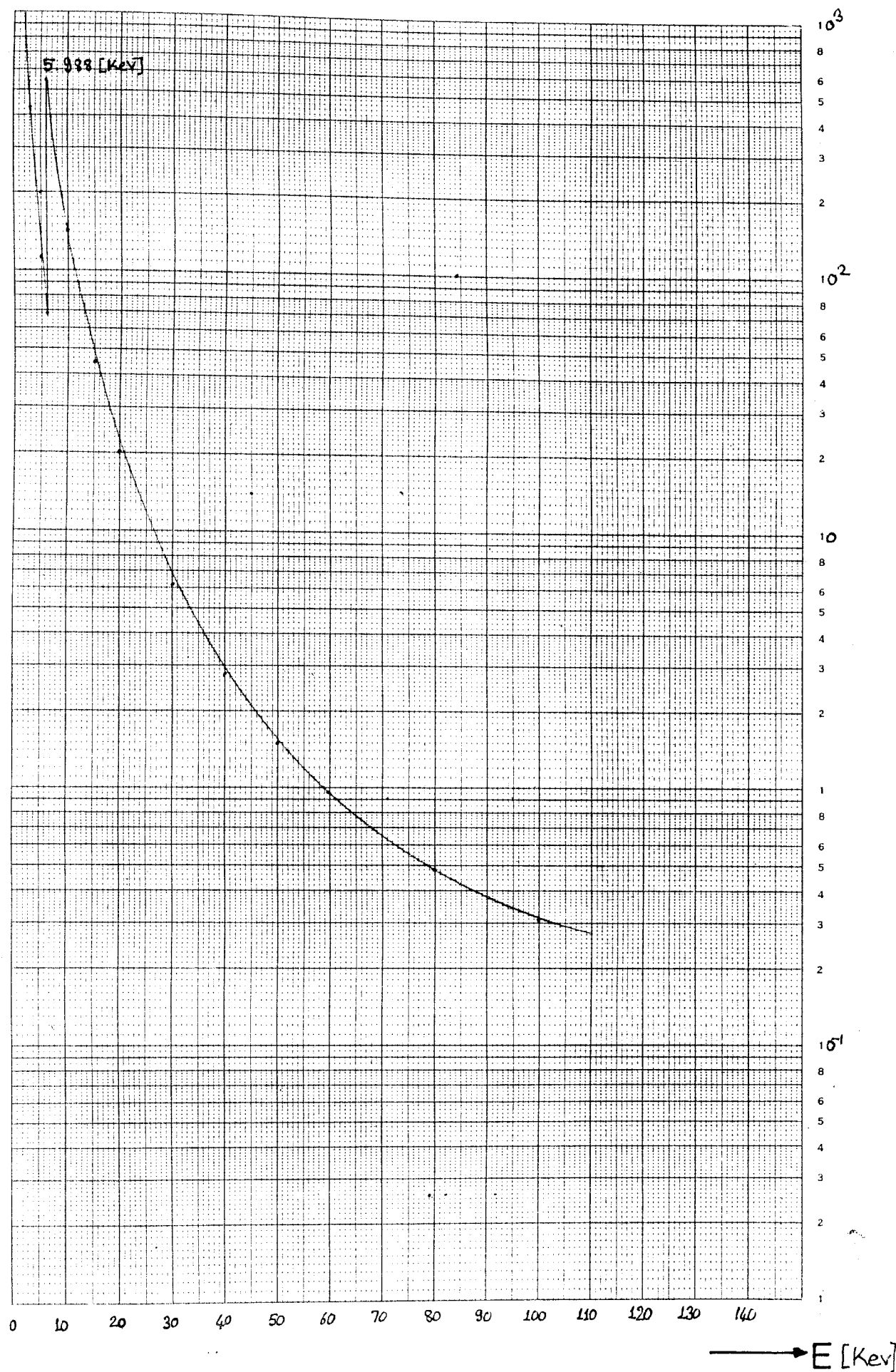
T.M.A.C. for Fe



→ E [keV]

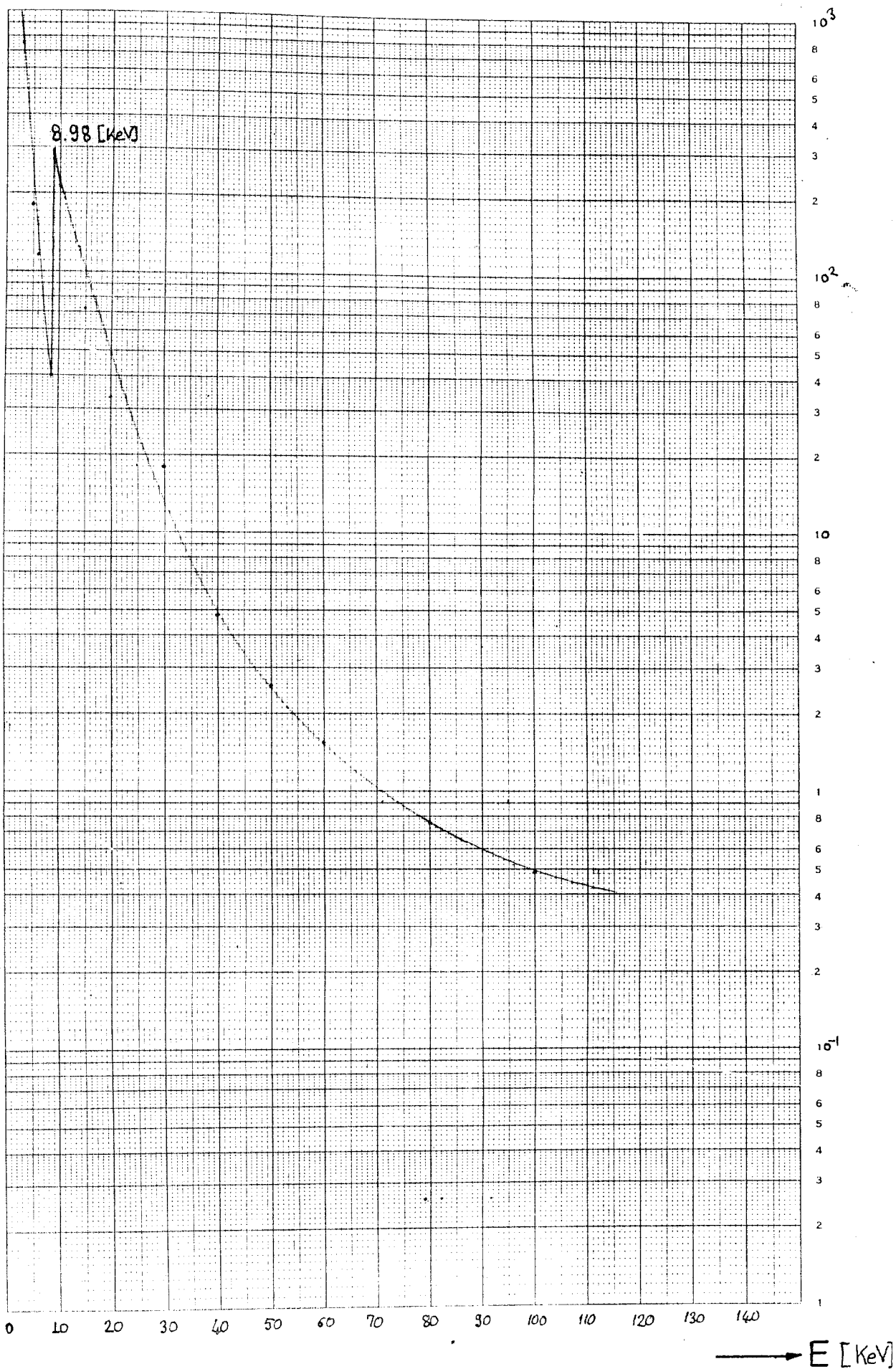


I.M.A.C. for Cr

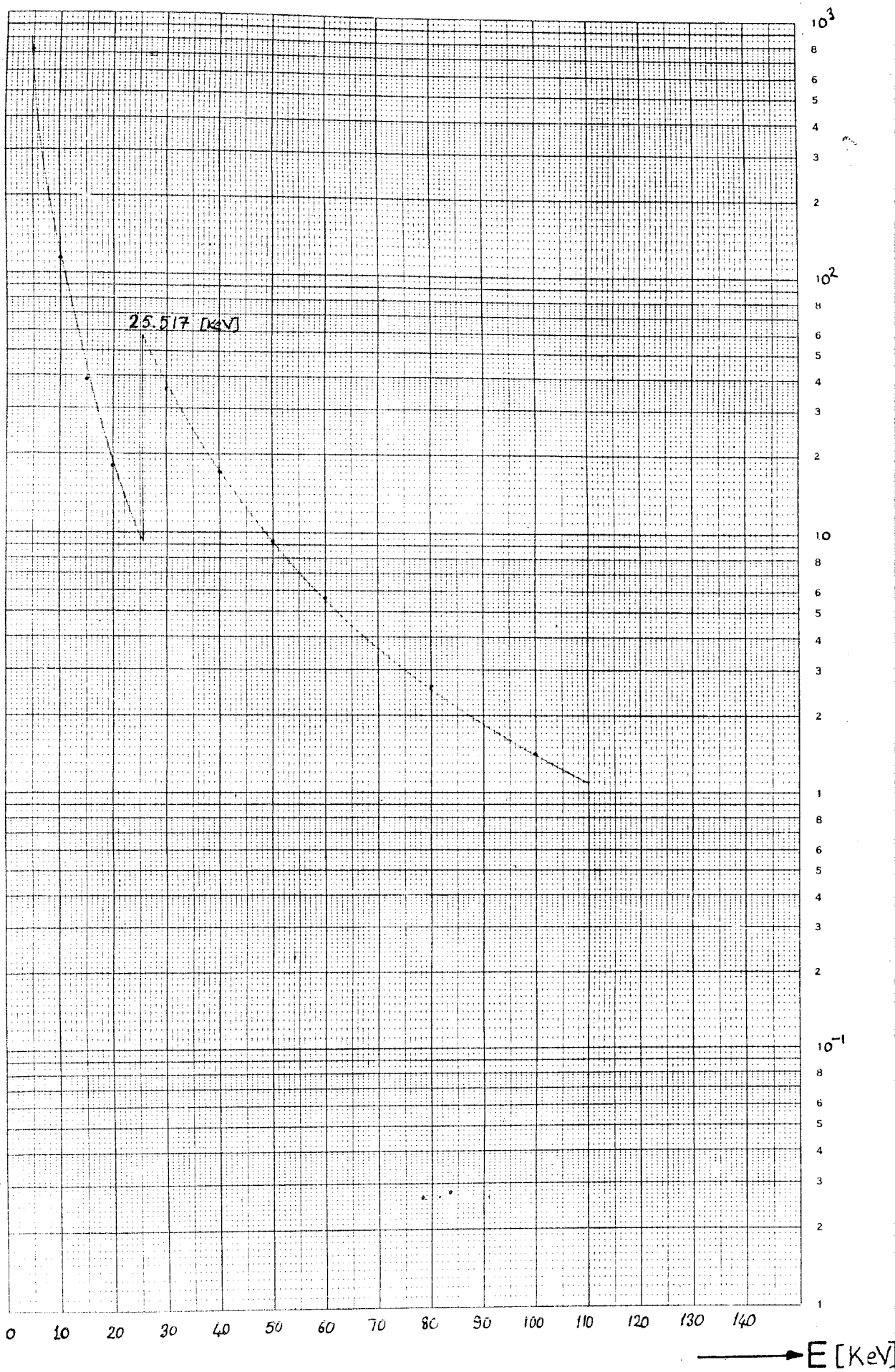


→ E [Kev]

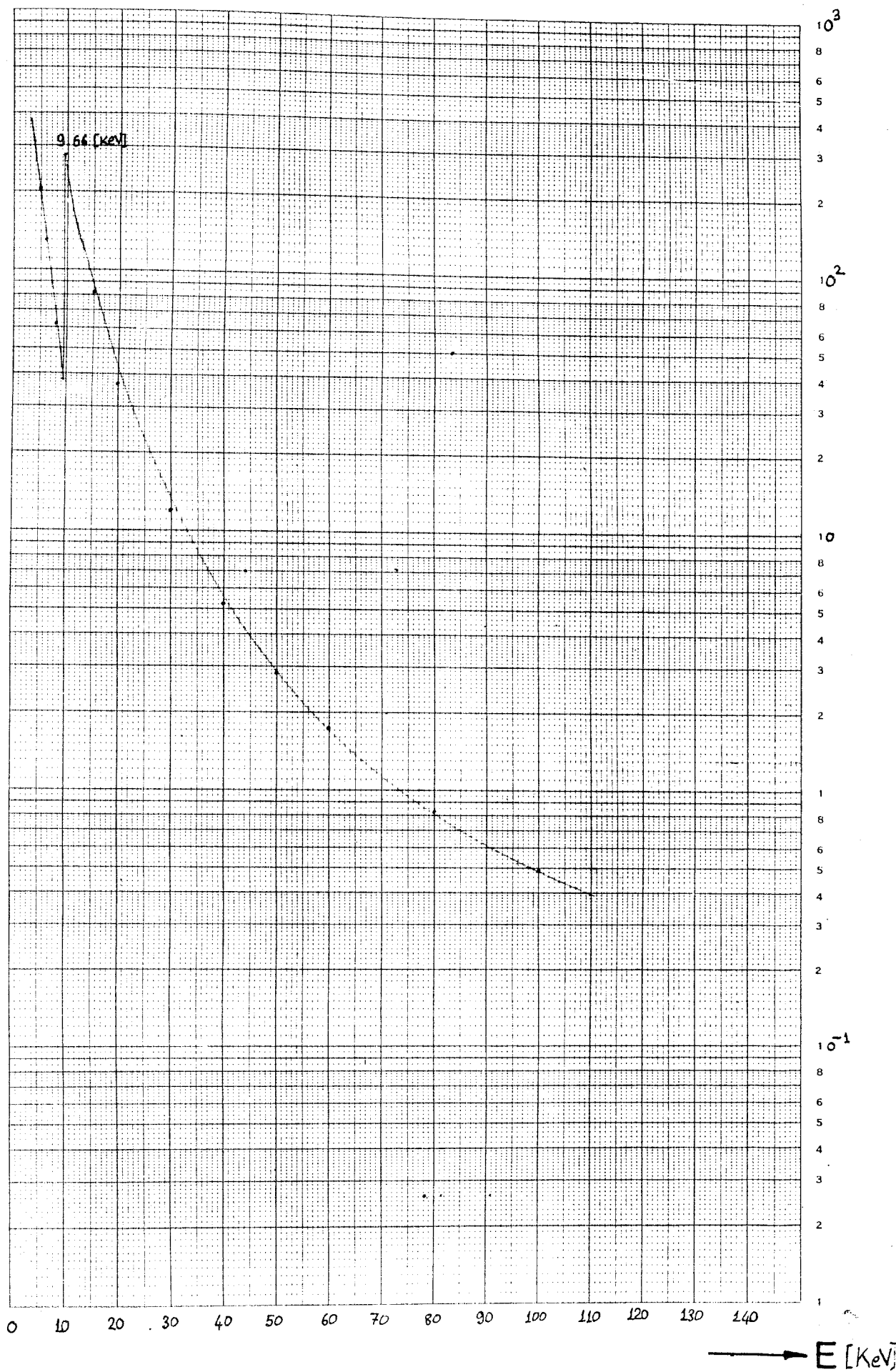
T.M.A.C. for Cu



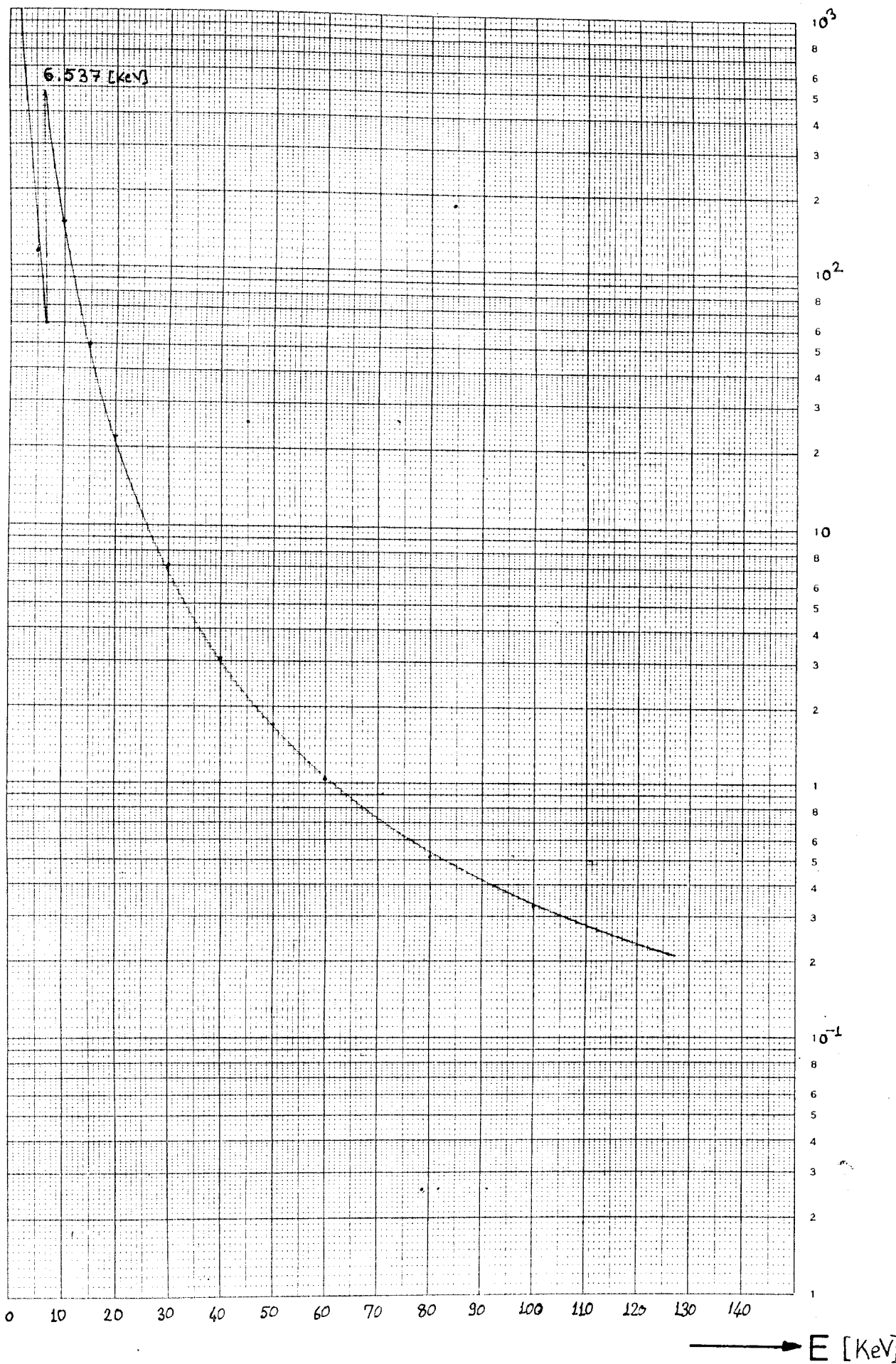
T.M.A.C. for Ag



T.M.A.C. for Zn



T.M.A.C. for Mn



## REFERENCES

- [Bi-77] Bilge, A. Nezihi. "Radyoizotop teknikleri ile analiz ve kaplama kalınlığı ölçümü" Cekmece nükleer araştırma ve eğitim merkezi yayınları. yayın no:1 , 1977.
- [Ga-67] Gardner, P. Robin. Radioisotope measurement applications in engineering. New York: Reinhold Publishing Co, Inc., 1967.
- [Ge-67] Gerald, J. Hine., "Instrumentation in nuclear medicine" Academic press, Vol.1. New York, 1967.
- [Gl-55] Glasstone Samuel, Sesonske Alexander. Nuclear reactor engineering. New York: D. Van Nostrand Company, Inc., 1955.
- [Go-56] Goldstein, Herbert. Fundamental aspects of reactor shielding. Massachusetts: Addison Wesley publishing Co, Inc., 1956.
- [Gr-67] Grafton, D. Chahe. Principles of radioisotope methodology. 3rd ed. Minneapolis: Burgess Publishing Co, 1967.
- [Hu-82] Hubbell, J. H "Photon mass attenuation and energy absorption coefficients from 1 KeV to 20 MeV" Journal of Applied Radiat. Isot., Vol.33. pp.1269 to 1290, 1982.
- [Ka-64] Kaplan, Irving. Nuclear Physics. 2nd. ed. Massachusetts: Addison Wesley Publishing Co, Inc., 1964.

- [Kn-79] Knoll, Glenn. Radiation detection and measurement  
New York: John Wiley and sons, Inc., 1979.
- [Ko-61] Kohl, Jerome. Radioisotope applications engineering.  
New York: D. Van Nostrand Company, Inc., 1961.
- [Le-74] Leaver, R.H. Analysis and Presentation of  
Experimental Results. London: The Macmillan  
Press LTD., 1974.
- [Le-68] Lederer, C. Michael., Hollander, M. Jack. Table of  
Isotopes. 6th. ed. New York: John Wiley and  
sons, Inc., 1968.
- [Ro-57] Rochlin, S. Robert., "Industrial users of radio  
isotopes" Nuclear electric review, November, 1957.
- [Sp-72] Spiegel, R. Murray. Statistics. New York:  
Mc Graw-Hill Book Company, Inc., 1972.
- [Se-65] Segre, Emilio. Nuclei and Particles New York:  
W.A. Benjamin, Inc., 1965.